Electronic Structure of Vanadium Oxide. Neutral and Charged Species, $VO^{0,\pm}$

Evangelos Miliordos and Aristides Mavridis*

Laboratory of Physical Chemistry, Department of Chemistry, National and Kapodistrian University of Athens, P.O. Box 64 004, 157 10 Zografou, Athens, Greece

Received: November 10, 2006

The diatomic molecule vanadium oxide, VO, and its charged species VO^+ and VO^- were studied by multireference and coupled cluster methods in conjunction with large basis sets. The investigation of 22 states and the construction of 21 full potential energy curves allowed for a detailed understanding of the electronic structure of these species. Our best binding energies for the ground states of VO ($X^4\Sigma^-$), VO^+ ($X^3\Sigma^-$), and VO^- ($X^3\Sigma^-$) were D_e = 150, 138, and 143 kcal/mol, respectively, in harmony with the corresponding experimental values. For both species VO and VO^+ and for all states studied, the bonding showed a strong ionic character conforming to the models V^+O^- and $V^{2+}O^-$.

1. Introduction

In an ongoing effort to elucidate the electronic structure of the diatomic 3d-transition metal-containing molecules, we present high-level ab initio calculations on the vanadium monoxide, VO, as well as on the ions VO^+ and VO^-. We have been motivated by the fact that VO is experimentally one of the most extensively studied systems among the MO oxides (M = Sc−Cu), whereas theoretical investigations are rather limited. Moreover, VO seems to be of both industrial and astrophysical importance.[1,2]

Practically all existing experimental and theoretical works on VO are collected in Table 1, whereas Tables 2 and 3 are analogous lists for the charged species, $VO^\pm$.

As early as 1935 Mahanti recorded the rotational spectrum of VO, suggesting a ground state of $^2\Delta$ symmetry and a dissociation energy D_0 = 147.6 kcal/mol obtained by linear Birge−Sponer extrapolation.[3] More than 20 years later Lagerqvist et al. using emission spectroscopy reported a D_0 = 143.9 kcal/mol and r_e = 1.589 Å for a quartet or a doublet state.[4] Experimentally the ground state of VO was unequivocally determined to be of symmetry $^4\Sigma$ by Kasai through ESR spectroscopy in frozen argon matrices.[7] The best experimental dissociation energy of the $X^4\Sigma^-$ state of VO so far seems to be D_0 = 149.5 ± 2 kcal/mol obtained by high-temperature mass spectrometry,[12] whereas most of the experimental work on the excited states of VO has been done by Merer and co-workers.[13,16] By employing high-resolution Fourier transform spectroscopy these workers report spectroscopic constants and separation energies (T_o) for the ground and a series of excited states of VO, namely $X^4\Sigma^-$, $A'^4\Phi$, $1^2\Delta$, $A^4\Pi$, $\alpha^2\Sigma^+$, $B^4\Pi$, $1^2\Phi$, $C^4\Sigma^-$, $1^2\Pi$, $2^2\Pi_{3/2}$, $D^4\Delta$, $2^2\Delta$ (Table 1).[13,16] It is interesting, however, that the first excited state of $^2\Sigma^-$ symmetry (not reported by Merer and co-workers[13,16]) was only recently detected by photoelectron spectroscopy.[15]

The first theoretical work on VO is the Hartree−Fock calculations of Carlson and Moser in 1966,[17] and the first modern post Hartree−Fock calculations on VO were done by Bauschlicher and Langhoff 20 years later.[18] For the $X^4\Sigma^-$ and $A'^4\Phi$, $1^2\Delta$, $A^4\Pi$ states these authors report dissociation energies and certain spectroscopic parameters at the CISD (configuration interaction + singles + doubles) and CPF (coupled pair functional)/[8s6p4d3f/$_V$ 6s4p3d1f/$_O$] level of theory. In addition, Bauschlicher and Maitre[20] examined by ACPF (averaged CPF) and RCCSD(T) (coupled cluster + singles + doubles + perturbative triples) methods the ground states of diatomic oxides (MO) and sulfides (MS), M = Sc−Cu. The most recent and extensive ab initio calculations on VO are those of Pykavy and van Wüllen who examined the $X^4\Sigma^-$ state of VO (and the X-states of $VO^\pm$) at the multireference-ACPF level using extended basis sets.[24] The rest of the theoretical results shown in Table 1 are at the density functional theory (DFT) level.[21−24]

Almost all existing experimental and theoretical results on the ground states of the charged species $VO^+(X^3\Sigma^-)$ and $VO^-(X^3\Sigma^-)$ are listed in Tables 2 and 3, respectively. Results either experimental or theoretical on the excited states of VO^+ or VO^- are, indeed, very limited (vide infra).

Using high-temperature photoelectron spectroscopy, Dyke et al. determined that the ground state of VO^+ is of $^3\Sigma^-$ symmetry.[26] Their D_0 value of 137.9 ± 2.3 kcal/mol is in good agreement with the guided ion beam mass spectrometry values of 134 ± 4 kcal/mol obtained 6 years later.[28] Dyke et al. determined also the vertical ionization energies (IE) for the transitions $VO(X^4\Sigma^-) \rightarrow VO^+(X^3\Sigma^-)$ and $VO(X^4\Sigma^-) \rightarrow VO^+(^3\Delta)$, IE = 7.25 ± 0.01 and 8.42 ± 0.01 eV, respectively.[26] In addition, a broad band observed at 11.41 ± 0.02 eV was associated with the transitions $VO(X^4\Sigma^-) \rightarrow VO^+(^5\Sigma^-,^5\Pi)$.

The only experimental results on VO^- are those of Wu and Wang obtained by photoelectron spectroscopy.[15] For the ground state, erroneously assigned as $^5\Pi$ instead of $^3\Sigma^-$, they give the harmonic frequency (ω_e) and the adiabatic IE of VO^- (or the electron affinity (EA) of VO), IE = 1.229 ± 0.008 eV. From the latter and the relation $D_0(VO^-;X^3\Sigma^-) = D_0(VO;X^4\Sigma^-) + EA(VO;X^4\Sigma^-) - EA(O;^3P)$, we can estimate the dissociation energy of VO^-: $D_0(VO^-;X^3\Sigma^-) = (6.483 \pm 0.088)^{12} + (1.229 \pm 0.008)^{15} - 1.4611^{35} = 6.251 \pm 0.096$ eV = 144.2 ± 2.2 kcal/mol. Wu and Wang recorded as well an excited state of VO^- of unknown symmetry located 6400 ± 200 cm^{-1} above its X-state.[15]

Motivated from the rather "scattered" theoretical data on $VO^{0,\pm}$ and the interest by the experimentalists in the 3d-metal oxides, we have performed multireference and coupled cluster calculations in conjunction with large basis sets with the purpose

* Corresponding author. E-mail address: mavridis@chem.uoa.gr.

10.1021/jp067451b CCC: $37.00
Published on Web 02/22/2007

TABLE 1: Experimental and Theoretical Results from the Literature for the VO Molecule [Dissociation Energies D (kcal/mol), Bond Distances r (Å), $\Delta G_{1/2}$ Values and Harmonic Frequencies ω_e (cm^{-1}), Dipole Moments μ (Debye), and Energy Separations T (cm^{-1})]

Experiment

state	D_0	r_o	$\Delta G_{1/2}$	μ	T_o	ref
?[a]	147.6					3
?[b]	143.9	1.589(=r_e)	1011.6(=ω_e)			4
?[c]	147.6 ± 4.6					5
X-state[c]	148.8 ± 2.5					6
$X^4\Sigma$[d]						7
X-state[c]	146.2 ± 4.0					8
X-state[e]	147.0−148.8					9
$X^4\Sigma^-$ [f]	≥139.2					10
X-state[g]	148.4 ± 4.0					11
$X^4\Sigma^-$ [h]	149.5 ± 2.0					12
$X^4\Sigma^-$ [i]		1.5921	1001.81	3.355(14)[j]	0.0	13
$\alpha^2\Sigma^-$ [k]			1090 ± 80		5630 ± 80	15
$A'^4\Phi$[i]		1.6286	936.48		7254.951	13
$1^2\Delta$[i]		1.5845	?1019.9		9374 ± 90[l]	13
$A^4\Pi$[i]		1.6368	884		9498.878[m]	13
$a^2\Sigma^+$ [n]		1.5856	1024.24		10412.46	16
$B^4\Pi$[i]		1.644	901		12605.57[o]	13
$1^2\Phi$[i]		1.6335			14920 ± 90[p]	13
$C^4\Sigma^-$ [i]		1.6747	852.6		17420.103	13
$1^2\Pi$[i]		1.6321	927.14		16582 ± 90[q]	13
$2^2\Pi_{3/2}$[i]		1.6219			17501 ± 90[r]	13
$D^4\Delta$[i]		1.6863	835		19148.08	13
$2^2\Delta$[i]		1.6828			24516 ± 90	13

Theory

state	D_e	r_e	ω_e	μ_e	T_e	ref
$X^4\Sigma^-$ [s]	109.8	1.574	1483	3.61	0.0	17
$X^4\Sigma^-$ [t]	131.0	1.604	959	2.50	0.0	18
$X^4\Sigma^-$ [u]		1.565	1083	2.99	0.0	18
$X^4\Sigma^-$ [v]	122.7	1.578	890		0.0	19
$X^4\Sigma^-$ [w]	131.4	1.598	993		0.0	20
$X^4\Sigma^-$ [x]	141.4	1.602	1028	3.60	0.0	20
$X^4\Sigma^-$ [y]	151−180	1.58−1.60	993−1045	3.55−3.74	0.0	21
$X^4\Sigma^-$ [z]		1.586	1028		0.0	22
$X^4\Sigma^-$ [aa]	159	1.569	1116		0.0	23
$X^4\Sigma^-$ [bb]	148.5	1.593	1035		0.0	24
$X^4\Sigma^-$ [cc]	143/172	1.58/1.585	1065/1043		0.0	24
$A'^4\Phi$[t]		1.652	857	2.67	6956	18
$A'^4\Phi$[u]		1.603	1062	3.47	7753	18
$A'^4\Phi$[z]		1.626	965		5886	22
$1^2\Delta$[t]		1.633	902	5.39	20809	18
$1^2\Delta$[u]		1.596	1041	7.13	22714	18
$A^4\Pi$[u]		1.642	934	7.34	11368	18
$A^4\Pi$[z]		1.619	969		11140	22
$B^4\Pi$[z]		1.648	935		10245	22

[a] First spectroscopic rotational analysis suggesting a ground state of (doubtful) $^2\Delta$ symmetry. D_0 obtained by linear Birge−Sponer extrapolation. [b] Emission spectroscopy giving evidence of a quartet or doublet of unknown spatial symmetry as quoted in ref 17. $D_0 \equiv D_e - \omega_e/2 = 145.3$ kcal/mol − 1011.6/2 cm^{-1} = 143.9 kcal/mol. [c] Thermochemical analysis of mass spectrometric data. [d] First unequivocal assignment of the electronic ground state by ESR spectroscopy in argon matrixes at 4 K. [e] As quoted in ref 8. [f] $C^4\Sigma^- - X^4\Sigma^-$ emission of VO produced under single collision conditions in the gas-phase reaction $V + NO_2 \rightarrow VO + NO$. [g] Thermochemical data. [h] High-temperature mass spectrometry. [i] High-resolution Fourier transform spectroscopy. [j] Reference 14, Fourier transform microwave spectroscopy. [k] Photoelectron spectroscopy. [l] Reference 2. Fourier transform emission spectroscopy. T_o value obtained indirectly from the relation $T_o(1^2\Delta) = T_o(1^2\Phi) - \Delta E(1^2\Phi \leftarrow 1^2\Delta) = 14920 \pm 90$ (ref 15) − 5546 (ref 2) = 9374 ± 90 cm^{-1}. [m] A value of $T_o = 9400 \pm 90$ is also given in ref 15. [n] Rotational analysis of Doppler-limited discharge emission spectroscopy. [o] A value of $T_o = 12500 \pm 90$ is also given in ref 15. [p] Reference 15. [q] T_o value obtained indirectly, $T_o(1^2\Pi) = T_o(1^2\Delta) + \Delta E(1^2\Pi \leftarrow 1^2\Delta)$ = 9374 ± 90 (see footnote *l*) + 7208.08 (ref 13) = 16582 ± 90 cm^{-1}. [r] T_o value obtained indirectly, $T_o(2^2\Pi_{3/2}) = T_o(1^2\Delta) + \Delta E(2^2\Pi_{3/2} \leftarrow 1^2\Delta)$ = 9374 ± 90 (see footnote *l*) + 8126.99 (ref 13) = 17501 ± 90 cm^{-1}. [s] Hartree−Fock calculations with a minimal + polarization complex Slater basis set. [t] Coupled pair functional (CPF)/[8s6p4d3f/$_V$ 6s4p3d1f/$_O$]. [u] CISD/[8s6p4d3f/$_V$ 6s4p3d1f/$_O$]. [v] CISD + Davidson correction/SEFIT pseudopotential + [6s5p3d1f] on V and [4s3p1d] on O. [w] Modified Coupled pair functional (MCPF)/[7s6p4d3f2g/$_V$ 6s5p4d3f1g/$_O$]. [x] RCCSD(T)/[8s6p4d2f/$_V$ 5s4p3d1f/$_O$]. The dipole moment is calculated at the UCCSD(T)/[8s6p4d2f/$_V$ 5s4p3d1f/$_O$] level. [y] DFT spread values depending on the functional used: BPW91, BLYP, and B3LYP/[6-311+G*]. [z] Time dependent DFT (B3LYP)/[6-311+G(2d)]. [aa] DFT (B3LYP)/[6-31G*]. [bb] MR-ACPF. D_e obtained through QZ-5Z CBS-limit. 5Z = [12s7p5d4f3g2h1i/$_V$ cc-pV5Z/$_O$]; ω_e and r_e values at the MR-ACPF/[8s5p3d2f1g/$_V$ cc-pVTZ/$_O$] level. [cc] DFT (B3LYP/BP86)/[8s5p3d2f1g/$_V$ cc-pVTZ/$_O$].

of better understanding the electronic structure and bonding of both neutral and charged VO species. For the VO, VO^+, and VO^- we have constructed a total of 21 potential energy curves reporting energetics, spectroscopic parameters, dipole moments (VO), spin−orbit couplings, and bonding characteristics.

2. Computational Approach

Two kinds of one electron basis sets were employed in the present study. For the V atom the atomic natural orbital (ANO) basis set of Bauschlicher[36] (20s15p10d6f4g) and for the O the

TABLE 2: Experimental and Theoretical Results from the Literature for the $X^3\Sigma^-$ State of VO^+ [Dissociation Energies D_0 (kcal/mol), Bond Distances r_e (Å) and Harmonic Frequencies ω_e (cm^{-1})]

ref	D_0	r_e	ω_e
		Experiment	
25[a]	131 ± 5		
26[b]	137.9 ± 2.3	1.54 ± 0.01	1060 ± 40
27[c]	138.4 ± 8.0		
28[a]	134 ± 4		
28[d]	138.1 ± 2.3		
29[e]			1053 ± 5
		Theory	
30[f]	117	1.56	1108
31	175[g]/156[h]	1.54[g]/1.56[h]	1146[g]/994[h]
32	131.7[i]	1.554[j]	1141[k]
33[l]	135 (134.5)	1.566 (1.571)	
33[m]	134.2	1.573	
33	128.2[n]/146.7[o]/148.0[p]	1.539[n]/1.559[o]/1.558[p]	
24[q]	136.3	1.563	1084
24[r]	127.3/150.0	1.538/1.548	1148/1117

[a] Guided ion beam mass spectrometry. [b] High-temperature photoelectron spectroscopy. [c] Low-energy collision-induced dissociation. [d] Obtained indirectly through the relation $D_0(VO^+) = D_0(VO) - IE(VO) + IE(V)$; D_0(VO) taken from ref 12 and IE(VO) from J. Harrington and J. C. Weisshaar (personal communication of the authors of ref 28). [e] Infrared photodissociation spectroscopy. [f] GVB-CI/[5s4p2d/$_V$ 4s2p1d/$_O$]. $D_0 = D_e - \omega_e/2$ and $E = -1016.59666$ E_h. [g] DFT(L). [h] DFT(NL). [i] MR-ACPF/[8s7p5d3f2g/$_V$ 6s5p3d/$_O$], $E = -1017.82994$ E_h. [j] DFT (ADF/BP). [k] B3LYP/6-311+G*. [l] MRCISD(+Q)/[Stuttgart relativistic small core effective potentials + 6s5p3d1f/$_V$ aug-cc-pVTZ/$_O$]. [m] MRMP (MCSCF + MP2)/same basis set as in footnote *l*. [n] DFT (B3LYP). [o] DFT (BLYP). [p] DFT (BOP)/same basis set as in footnote *l*. [q] MR-ACPF, same as footnote *bb* of Table 1. [r] DFT (B3LYP/BP86)/[8s5p3d2f1g/$_V$ cc-pVTZ/$_O$].

TABLE 3: Experimental and Theoretical Results from the Literature for the $X^3\Sigma^-$ State of VO^-

ref	D_0 (kcal/mol)	r_e (Å)	ω_e (cm^{-1})	IE (eV)
		Experiment		
15[a]			900 ± 50	1.229 ± 0.008
		Theory		
21[b]		1.604−1.619	960−991	0.81−1.09
34[c]		1.61/1.62		1.18/1.13
24[d]	128.9	1.626	957	
24[e]	146.2/170.2	1.602/1.607	1028/1007	

[a] Photoelectron spectroscopy. [b] DFT, see footnote *y* of Table 1. [c] DFT (B3LYP/BP86)/[6s4p3d/$_V$ 5s3p1d/$_O$]. [d] MR-ACPF, same as footnote *bb* of Table 1. [e] DFT (B3LYP/BP86)/[8s5p3d2f1g/$_V$ cc-pVTZ/$_O$].

augmented correlation consistent set of quadruple quality (aug-cc-pVQZ=AQZ) of Dunning[37] (13s7p4d3f2g) were used, both generally contracted to [7s6p4d3f2g/$_V$ 6s5p4d3f2g/$_O$]. This 164 spherical Gaussian basis set was used for the construction of all our potential energy curves (PEC). For the ground states of VO and $VO^{\pm}$ the newly developed valence correlation consistent Balabanov−Peterson (BP) basis set of quadruple-ζ quality (cc-pVQZ) for the V was also employed,[38] combined with the AQZ for the O atom generally contracted to [8s7p5d3f2g1h/$_V$ 6s5p4d3f2g/$_O$].

To construct potential energy curves for all states and species studied, the complete active space self-consistent field (CASSCF) plus single plus double replacements (CASSCF+1+2=MRCI) methodology was applied. The CASSCF zero-order wave functions were constructed by distributing 8 (VO^+), 9 (VO), and 10 (VO^-) "valence" electrons in 9 ($4s^V + 3d^V + 2p^O$), 11 ($4s^V + 3d^V + 4p_x^V + 4p_y^V + 2p^O$), and 9 ($4s^V + 3d^V + 2p^O$) orbitals, respectively. The inclusion of the active $2s^2$ electrons of the O atom in the active space was met with insurmountable technical problems; of course, these electrons were included in all subsequent MRCI calculations. Depending on the space-spin symmetry the CASSCF expansions range from 14 500 ($X^4\Sigma^-$) to 19 010 ($a^2\Sigma^-$) configuration functions (CF) for the neutral VO, with MRCI valence spaces of about 0.95×10^9 CFs with the ANO-Bauschlicher (B) basis set.[36] The corresponding number for the $X^4\Sigma^-$ using the Balabanov−Peterson (BP) basis[38] is 1.25×10^9 CFs. By applying the internal contraction approximation (icMRCI)[39] the size of the CI spaces become 15.3×10^6 ($X^4\Sigma^-$) and 17.5×10^6 ($X^4\Sigma^-$), respectively, thus rendering the calculations tractable.

To account for the semicore ($3s^23p^6$) correlation effects, icMRCI calculations were performed by including the $3s^23p^6$ electrons of the V atom in the CI procedure. For these calculations both sets, the B and BP were used, but note that the former does not contain specially tuned core functions. For the latter (BP), the weighted-core cc-pwCVQZ basis set by Balabanov and Peterson[38] was employed contracted to [10s9p7d4f3g2h]. We will refer to these calculations as C-MRCI. The size of the C-MRCI expansions for the VO species are $(17-18) \times 10^9$ CFs reduced to about 300×10^6 CFs after applying the internal contraction approximation. To reduce further their size, configuration functions with coefficients smaller than 10^{-3} were excluded from the CASSCF reference functions, resulting in icC-MRCI expansions ranging from 60 to 80×10^6 CFs and CASSCF norms of about 0.999. For the VO^+ and VO^- species there was no need to slice down the CASSCF reference spaces.

To corroborate our MRCI results, states $X^4\Sigma^-$, $1^2\Delta$ of VO, $X^3\Sigma^-$, $^3\Delta$, $^5\Pi$, $^5\Sigma^-$ of VO^+, and $X^3\Sigma^-$, $^5\Pi$ of VO^- were also examined around equilibrium with the restricted coupled cluster method including single and double excitations along with a noniterative estimate of connected triples, based on a restricted Hartree−Fock reference function, RCCSD(T),[40] and with both basis sets B and BP. RCCSD(T) calculations including the $3s^23p^6$ electrons of V will be referred to as C-RCCSD(T).

Scalar relativistic effects for all states studied were taken into account through the second order Douglas−Kroll−Hess (DKH2) approach[41] for C-MRCI and C-RCCSD(T) wave functions. For the DKH2 calculations the appropriately contracted BP[38] basis set cc-pwCVQZ-DK was used in conjunction with the uncontracted AQZ basis set of the O atom.[37]

Spin−orbit effects (SO) were obtained by diagonalizing the Breit−Pauli operator at the MRCI/[cc-pVQZ/$_V$ AQZ/$_O$] level.

Basis set superposition errors (BSSE)[42] were estimated for the ground state of VO($X^4\Sigma^-$), VO^+($X^3\Sigma^-$), and VO^-($X^3\Sigma^-$) and for both B/BP basis sets. For VO, VO^+, and VO^- BSSEs at the MRCI (C-MRCI) level of theory are (in kcal/mol): 0.43 (3.39)/0.42 (0.45), 0.35 (3.52)/0.34 (0.48), and 0.46 (3.25)/0.45 (0.49). The corresponding numbers at the RCCSD(T) (C-RCCSD(T)) level are: 0.56 (3.68)/0.68 (0.70), 0.45 (3.91)/0.57 (0.58), and 0.63 (3.75)/0.57 (0.77). Note that whereas the BSSE is practically the same at the MRCI and RCCSD(T) for both basis sets, B or BP, at the C-MRCI and C-RCCSD(T) levels, Bauschlicher's (B) basis set gives BSSEs of about an order of magnitude larger than the corresponding ones with the Balabanov−Peterson (BP) basis set due to the formers' lack of $3s^23p^6$ core functions.

All calculations were done under C_{2v} symmetry constraints; nevertheless all CASSCF wave functions possess correct spatial angular momentum symmetry. However, MRCI or C-MRCI wave functions display the symmetry of the C_{2v} species, A_1 (or A_2) and B_1 (or B_2). In addition, all excited states of VO and

TABLE 4: Ionization Energies IE (eV) of V (a ^{4}F), Atomic Energy Separations of $V^+(^5D)$ $^5F \leftarrow {}^5D$ and $^3F \leftarrow {}^5D$ (eV), and Electron Affinities EA (eV) of the $O(^3P)$ Atom in Different Methodologies

method[a]	IE	$^5F \leftarrow {}^5D$	$^3F \leftarrow {}^5D$	EA
MRCI[b]	6.47	0.382	1.068	1.18
MRCI+Q[b]	6.52	0.399	1.066	1.37
MRCI+DKH2[b]	6.73	0.152	0.863	1.06
MRCI+DKH2+Q[b]	6.78	0.169	0.861	1.29
C-MRCI[b]	6.37	0.388	1.208	
C-MRCI+Q[b]	6.49	0.438	1.213	
C-MRCI+DKH2[b]	6.64	0.134	0.987	
C-MRCI+DKH2+Q[b]	6.77	0.182	0.984	
RCCSD(T)[b]	6.49	0.394		1.40
C-RCCSD(T)[b]	6.50	0.470		
RCCSD(T)+DKH2[b]	6.78	0.159		1.40
C-RCCSD(T)+DKH2[b]	6.81	0.224		
MRCI[c]	6.53	0.365	1.006	
MRCI+Q[c]	6.53	0.415	1.048	
MRCI+DKH2[c]	6.81	0.143	0.813	
MRCI+DKH2+Q[c]	6.81	0.194	0.855	
C-MRCI[c]	6.43	0.375	1.132	
C-MRCI+Q[c]	6.45	0.471	1.231	
C-MRCI+DKH2[c]	6.70	0.149	0.935	
C-MRCI+DKH2+Q[c]	6.73	0.243	1.030	
RCCSD(T)[c]	6.49	0.387		
C-RCCSD(T)[c]	6.47	0.495		
RCCSD(T)+DKH2[c]	6.77	0.165		
C-RCCSD(T)+DKH2[c]	6.75	0.268		
expt	6.74[d]	0.337[d,e]	1.079[d,e]	1.46[f]

[a] Internally contracted MRCI and C-MRCI calculations. +Q and DKH2 refer to the Davidson correction and to second-order Douglas–Kroll–Hess scalar relativistic corrections. [b] Bauschlicher basis set for V, see text. [c] Balabanov–Peterson basis set for V, see text. [d] Reference 45. [e] M_J averaged values. [f] Reference 35.

VO^+ were obtained through the state average (SA) approach.[43] Finally, size extensivity effects at the MRCI (C-MRCI) level are about 5 (21), 8 (23), 14 (36) mE_h for VO^+, VO, and VO^-, respectively, reduced to 1.5 (4), 4 (7), and 6 (16) at the MRCI+Q (C-MRCI+Q) level, where Q is the Davidson correction for unlinked quadruples.

All calculations were performed by the MOLPRO2002.6 and MOLPRO2006.1 programs.[44]

3. Results and Discussion

Table 4 lists the ionization energy (IE) of V, $V(^4F;4s^23d^3) \rightarrow V^+(^5D;3d^4)$, and the atomic separation energies $\Delta E(^5F \leftarrow {}^5D, {}^3F \leftarrow {}^5D)$ of V^+ in a variety of methodologies and the two basis sets, B and BP. Observe that a good agreement between experimental and theoretical IEs is only obtained after correcting for relativity at all levels of theory. However, DKH2 corrections do not help in improving the first two $^5F \leftarrow {}^5D$, $^3F \leftarrow {}^5D$ energy splittings of V^+, with the best results obtained at the MRCI level.

A. VO. The ground states of $V(^4F)$ and $O(^3P)$ atoms give rise to 36 molecular states, namely $\Gamma[1]$, $\Phi[2]$, $\Delta[3]$, $\Pi[3]$, $\Sigma^+[2]$, $\Sigma^{-1}[1]$ doublets, quartets, and sextets. We have examined the first lowest nine states, i.e., $X^4\Sigma^-$, $\alpha^2\Sigma^-$, $A'^4\Phi$, $1^2\Delta$, $1^2\Gamma$, $A^4\Pi$, $\alpha^2\Sigma^+$, $B^4\Pi$, and $1^2\Phi$ following the experimental notation. With the exception of the $1^2\Gamma$ state, which is reported here for the first time, the rest of the states have been detected experimentally (Table 1). Figure 1 displays their PECs at the valence MRCI/[B/$_V$ AQZ/$_O$] level, whereas all numerical results are collected in Table 5. Table 6 lists leading CASSCF CFs along with Mulliken CASSCF and MRCI equilibrium atomic distributions. All states correlate adiabatically to the ground state atoms, $V(^4F) + O(^3P)$; nevertheless their equilibrium structure

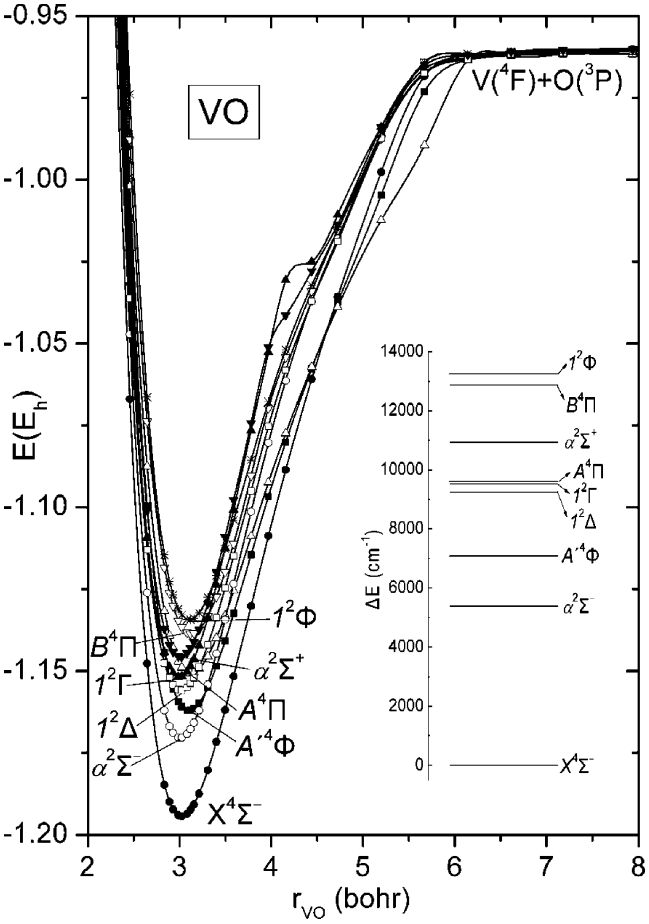

Figure 1. MRCI+Q potential energy curves and energy levels (inset) of VO. All energies are shifted by +1017.0 hartree.

shows clearly a strong ionic component, V^+O^-. With the V^+O^- structure, ionic avoided crossings are expected around 27.2/[IE(V) − EA(O)] = 27.2/(6.7 − 1.5) = 5.2 bohr, and indeed this is the case as depicted in Figure 1. In addition, dipole moments change dramatically at about this internuclear distance as the two atoms come closer, from zero ($r_{VO} = \infty$) to almost 10 Debye (r_{VO} = 5.5 bohr), a strong indication of the V^+O^- participation in the bond formation.

The question is now to what states of V^+ our calculated nine states correlate *diabatically*. From the first three states of V^+ $^5D_g(3d^4)$, $^5F_g(4s^13d^3)$, and $^3F_g(4s^13d^3)$ interacting with the $^2P_u(2p^5)$ state of O^-, one obtains three groups of molecular states $^{4,6}\{\Phi[1], \Delta[2], \Pi[3], \Sigma^+[2], \Sigma^-[1]\}$, $^{4,6}\{\Gamma[1], \Phi[2], \Delta[3], \Pi[3], \Sigma^+[1], \Sigma^-[2]\}$, and $^{2,4}\{\Gamma[1], \Phi[2], \Delta[3], \Pi[3], \Sigma^+[1], \Sigma^-[2]\}$, respectively. Because of spin-angular momentum symmetry, the doublets $\alpha^2\Sigma^-$, $1^2\Gamma$, $\alpha^2\Sigma^+$, $1^2\Phi$ can only correlate to a triplet V^+ term + $O^-(^2P_u)$; the $1^2\Delta$ is an exception, being rather of covalent or less ionic nature. As our population analysis indicates (see Table 6), states $\alpha^2\Sigma^-$ and $1^2\Phi$ should correlate *diabatically* to $V^+(^3F_g) + O^-(^2P_u)$, and $1^2\Gamma$, $\alpha^2\Sigma^+$ to $V^+(b^3G(4s^13d^3)) + O^-(^2P_u)$ (vide infra). Following again the Mulliken distributions on the in situ V^+ ion, $B^4\Pi$ should correlate to $V^+(^5D_g) + O^-(^2P_u)$, whereas the rest of the quartets, $X^4\Sigma^-$, $A'^4\Phi$, $A^4\Pi$, with an in situ V^+ $4s^13d^3$ distribution (Table 6), should correlate to $V^+(^5F_g) + O^-(^2P_u)$.

$X^4\Sigma^-$. A single configuration describes adequately the ground state of VO around equilibrium as shown in Table 6. The CASSCF and MRCI Mulliken population analysis points clearly to an ionic equilibrium structure with a transfer of about 0.5 e^- from V to O. As was previously discussed, the $X^4\Sigma^-$ state of

TABLE 5: Total Energies E (hartree), Equilibrium Bond Distances r_e (Å), Dissociation Energies D_e (kcal/mol), $\Delta G_{1/2}$ Values (cm^{-1}) and Anharmonicities $\omega_e x_e$ (cm^{-1}), Rotational−Vibrational Constants a_e ($\times 10^{-3}$ cm^{-1}), Dipole Moments μ_e (D), and Energy Separations T_e (cm^{-1}) of the Neutral VO Molecule

method[a]	$-E$	r_e	D_e[b]	$\Delta G_{1/2}$	$\omega_e x_e$	a_e	$\langle\mu\rangle/\mu_{FF}$[c]	T_e
			$X^4\Sigma^-$					
CASSCF/B	1017.92188	1.612	129.8	972	5.7	3.5	2.43/2.43	0.0
MRCI/B	1018.17708	1.599	147.6	982	5.3	3.4	2.79/3.28	0.0
MRCI+Q/B	1018.19412	1.600	148.7	978	5.6	3.4	/3.37	0.0
MRCI/BP	1018.17966	1.599	148.5	983	6.4	3.7	2.61/3.09	0.0
MRCI+Q/BP	1018.19563	1.605	148.7	980	6.3	3.3	/3.22	0.0
C-MRCI/B	1018.47912	1.591	153.4	998	4.2	3.5	2.54/3.11	0.0
C-MRCI+Q/B	1018.53218	1.594	155.0	989	4.6	3.3	/3.28	0.0
C-MRCI/BP	1018.53764	1.589	150.8	997	5.7	2.4	2.43/3.00	0.0
C-MRCI+Q/BP	1018.59531	1.592	152.9	992	6.0	2.5	/3.23	0.0
C-MRCI+DKH2/BP	1023.83898	1.588	150.1	1006	8.1	3.8	2.52/3.10	0.0
C-MRCI+DKH2+Q/BP	1023.89668	1.591	151.7	1002	7.4	3.9	/3.26	0.0
RCCSD(T)/B	1018.19410	1.596	146.0	1024	6.3	3.6	/3.39	0.0
C-RCCSD(T)/B	1018.54132	1.586	152.4	1033	3.9	3.1	/3.36	0.0
RCCSD(T)/BP	1018.19525	1.595	146.2	1025	3.5	3.1	/3.30	0.0
C-RCCSD(T)/BP	1018.60646	1.585	149.9	1039	3.4	2.8	/3.38	0.0
C-RCCSD(T)+DKH2/BP	1023.90805	1.583	149.2				/3.37	0.0
expt		1.589[d]	149.5 ± 2[e]	1001.81[d]			3.355 ± 0.014[f]	0.0
			$\alpha^2\Sigma^-$					
CASSCF/B	1017.89505	1.598	112.5	1003	5.7	3.5	0.82/0.82	5889
MRCI/B	1018.15136	1.591	131.0	1008	5.5	3.4	1.22/1.61	5643
MRCI+Q/B	1018.16958	1.591	133.1	1008	5.3	3.3	/1.75	5385
C-MRCI/B	1018.45269	1.584	135.8	1027	5.4	3.4	0.86/1.39	5800
C-MRCI+Q/B	1018.50563	1.586	137.9	1023	5.1	3.4	/1.66	5828
C-MRCI/BP	1018.51144	1.582	134.4	1036	8.7	3.3	0.74/1.27	5751
C-MRCI+Q/BP	1018.56882	1.583	136.1	1017	5.7	4.0	/1.54	5815
C-MRCI+DKH2/BP	1023.81069	1.579	132.8	1031	2.5	3.5	0.87/1.36	5992
C-MRCI+DKH2+Q/BP	1023.86813	1.582	134.4	1020	2.6	3.6	/1.62	6039
expt[g]			133.4 ± 2.2[h]	1090 ± 80				5630 ± 80
			$A'^4\Phi$					
CASSCF/B	1017.89054	1.656	109.5	900	5.9	3.5	3.13/3.12	6878
MRCI/B	1018.14433	1.639	126.4	913	5.6	3.4	3.25/3.59	7187
MRCI+Q/B	1018.16184	1.640	127.8	912	5.7	3.4	/3.60	7084
C-MRCI/B	1018.44266	1.630	129.8				3.05/	8001
C-MRCI+Q/B	1018.49708	1.631	132.6					7702
C-MRCI/BP	1018.50096	1.628	127.8				3.01/	8049
C-MRCI+Q/BP	1018.55999	1.638	130.3					7753
C-MRCI+DKH2/BP	1023.80174	1.627	127.5				3.13/	7956
C-MRCI+DKH2+Q/BP	1023.86086	1.639	130.3					7635
expt[i]		1.6286	128.8 ± 2[h]	936.48				7254.951
			$1^2\Delta$					
CASSCF/B	1017.85084	1.610	84.2	914	5.3	4.4	0.97/0.98	15591
MRCI/B	1018.12400	1.599	114.1	934	5.4	4.0	1.57/2.01	11649
MRCI+Q/B	1018.15198	1.595	122.2	952	5.3	3.7	/2.08	9248
C-MRCI/B	1018.42426	1.589	118.1				0.93/	12040
C-MRCI+Q/B	1018.48753	1.586	126.6					9799
C-MRCI/BP	1018.48150	1.587	115.3				0.82/	12321
C-MRCI+Q/BP	1018.54943	1.586	123.8					10071
C-MRCI+DKH2/BP	1023.78692	1.586	118.1				0.85/	11207
C-MRCI+DKH2+Q/BP	1023.85483	1.585	126.1					8957
RCCSD(T)/B	1018.15521	1.587	121.5	1009	5.4	3.5	/2.01	8535
C-RCCSD(T)/B	1018.50076	1.576	126.8				/1.81	8901
C-RCCSD(T)/BP	1018.56518	1.576	124.1	1021	5.4	3.4	/2.01	9059
C-RCCSD(T)+DKH2/BP	1023.87191	1.570	126.6					7932
expt		1.5845[i]	122.7 ± 2.3[h]	?1019.9[i]				9374 ± 90[j]
			$1^2\Gamma$					
CASSCF/B	1017.87639	1.592	100.3	1027	4.4	3.2	1.78/1.78	9983
MRCI/B	1018.13226	1.586	119.0	1025	4.6	3.3	2.13/2.59	9836
MRCI+Q/B	1018.15078	1.586	121.3	1025	4.6	3.2	/2.71	9512
C-MRCI/B	1018.43451	1.578	124.5				3.19/	9789
C-MRCI+Q/B	1018.49128	1.580	128.9					8976
C-MRCI/BP	1018.49376	1.576	123.1				3.18/	9629
C-MRCI+Q/BP	1018.55497	1.578	127.3					8854
C-MRCI+DKH2/BP	1023.79412	1.575	122.5				3.26/	9627
C-MRCI+DKH2+Q/BP	1023.85533	1.577	126.6					8849
			$A^4\Pi$					
CASSCF/B	1017.87699	1.669	101.0	846	5.5	3.8	3.07/3.07	9854
MRCI/B	1018.13233	1.650	118.8	866	5.4	3.6	3.62/3.84	9821
MRCI+Q/B	1018.15033	1.651	120.6	866	5.1	3.5	/3.90	9614
C-MRCI/B	1018.43079	1.639	122.5				3.59/	10606
C-MRCI+Q/B	1018.48803	1.641	127.1					9690
C-MRCI/BP	1018.48899	1.638	120.4				3.57/	10676
C-MRCI+Q/BP	1018.55122	1.639	125.2					9677
C-MRCI+DKH2/BP	1023.78937	1.637	119.7				3.55/	10669
C-MRCI+DKH2+Q/BP	1023.85170	1.639	124.5					9644
expt[i]		1.6368	122.3 ± 2[h]	884				9498.878

TABLE 5: Continued

method[a]	$-E$	r_e	D_e[b]	$\Delta G_{1/2}$	$\omega_e x_e$	a_e	$\langle\mu\rangle/\mu_{FF}$[c]	T_e
			$1^2\Sigma^+$					
CASSCF/B	1017.86066	1.602	90.9	999	5.3	3.2	3.63/2.40	13437
MRCI/B	1018.12415	1.592	113.9	1007	4.8	3.2	3.13/2.89	11615
MRCI+Q/B	1018.14424	1.592	117.1	1008	4.8	3.2	/2.76	10947
C-MRCI/B	1018.42315	1.587	117.6				3.24/	12284
C-MRCI+Q/B	1018.48290	1.587	123.8					10815
C-MRCI/BP	1018.48203	1.586	116.0				3.23/	12205
C-MRCI+Q/BP	1018.54619	1.587	122.0					10782
C-MRCI+DKH2/BP	1023.78241	1.586	115.3				3.32/	12198
C-MRCI+DKH2+Q/BP	1023.84659	1.587	121.3					10766
expt[i]		1.5856	119.7 ± 2[h]	1024.24				10412.46
			$B^4\Pi$					
CASSCF/B	1017.83420	1.706	75.2	824	9.8	3.4	7.52/7.59	19245
MRCI/B	1018.10990	1.662	105.6	870	4.5	2.5	6.45/6.39	14743
MRCI+Q/B	1018.13550	1.654	112.1	894	4.5	2.8	/5.74	12864
C-MRCI/B	1018.41144	1.652	110.5				6.73/	14852
C-MRCI+Q/B	1018.47123	1.645	116.7					13377
C-MRCI/BP	1018.46980	1.652	108.4				6.75/	14889
C-MRCI+Q/BP	1018.53384	1.644	114.4					13491
C-MRCI+DKH2/BP	1023.76582	1.650	104.9				6.82/	15839
C-MRCI+DKH2+Q/BP	1023.82976	1.643	110.9					14460
expt[i]		1.644	113.5 ± 2[h]	901				12605.57
			$1^2\Phi$					
CASSCF/B	1017.86015	1.656	90.6	916	5.9	3.6	2.26/2.26	13548
MRCI/B	1018.11513	1.646	108.4	932	5.7	3.4	2.72/3.21	13596
MRCI+Q/B	1018.13375	1.644	110.5	934	5.5	3.3	/3.31	13248
C-MRCI/B	1018.41413	1.637	112.1				2.43/	14263
C-MRCI+Q/B	1018.46817	1.636	114.6					14048
C-MRCI/BP	1018.47274	1.635	110.2				2.34/	14243
C-MRCI+Q/BP	1018.53127	1.634	112.5					14056
C-MRCI+DKH2/BP	1023.77218	1.634	109.1				2.49/	14444
C-MRCI+DKH2+Q/BP	1023.83081	1.633	111.4					14229
expt		1.6335[i]	106.8 ± 2.3[h]					14920 ± 90[g]

[a] Internally contracted MRCI and C-MRCI calculations. +Q and DKH2 refer to the Davidson correction and to second order Douglas–Kroll–Hess relativistic corrections. B and BP refer to Bauschlicher and Balabanov–Petterson basis sets on V; see text. [b] With respect to the ground state atoms $V(^4F) + O(^3P)$. [c] $\langle\mu\rangle$ calculated as an expectation value, μ_{FF} by the finite field method. Field intensity 10^{-5} au. [d] Reference 4. [e] D_o, ref 12. [f] Reference 14. [g] Reference 15. [h] "Experimental" D_0 value obtained by subtracting the experimental energy separation T_o from the experimental $D_0 = 144.5 \pm 2$ of the $X^4\Sigma^-$ state. [i] Reference 13. [j] See footnote *l* of Table 1.

TABLE 6: Dominant Equilibrium CASSCF Configurations, CASSCF and MRCI (in Parentheses) Mulliken Atomic Populations, and Total Charge (q_v) on the Vanadium Atom of the VO Molecule. Only "Valence" Electrons Are Counted.

		populations													
		V									O				
state	configurations	4s	$4p_z$	$4p_x$	$4p_y$	$3d_{z^2}$	$3d_{xz}$	$3d_{yz}$	$3d_{x^2-y^2}$	$3d_{xy}$	2s	$2p_z$	$2p_x$	$2p_y$	q_v
$X^4\Sigma^-$	$0.93\lvert 1\sigma^2 2\sigma^2 3\sigma^1 1\pi_x^2 1\pi_y^2 1\delta_+^1 1\delta_-^1\rangle$	0.93	0.11	0.01	0.01	0.64	0.38	0.38	0.99	0.99	1.89	1.41	1.59	1.59	0.52
		(0.91	0.10	0.01	0.01	0.64	0.39	0.39	0.98	0.98	1.90	1.42	1.57	1.57	0.54)
$a^2\Sigma^-$	$\lvert 1\sigma^2 2\sigma^2 3\sigma^1 1\pi^4[0.81(\overline{1\delta_+^1 1\delta_-^1}) + 0.47(1\delta_+^1\overline{1\delta_-^1})]\rangle$	0.95	0.18	0.01	0.01	0.60	0.38	0.38	0.99	0.99	1.88	1.38	1.59	1.59	0.48
		(0.95	0.16	0.02	0.02	0.59	0.39	0.39	0.98	0.98	1.88	1.39	1.57	1.57	0.49)
$A'^4\Phi$	$0.66\lvert 1\sigma^2 2\sigma^2 3\sigma^1 1\pi_x^2 1\pi_y^2(2\pi_x^1 1\delta_+^1 - 2\pi_y^1 1\delta_-^1)\rangle$	0.93	0.12	0.05	0.05	0.65	0.78	0.78	0.50	0.50	1.90	1.38	1.64	1.64	0.60
		(0.91	0.10	0.07	0.07	0.65	0.78	0.78	0.50	0.50	1.91	1.40	1.62	1.62	0.61)
$1^2\Delta$	$0.92\lvert 1\sigma^2 2\sigma^2 3\sigma^2 1\pi_x^2 1\pi_y^2 1\delta_+^1\rangle$	1.56	0.07	0.08	0.08	0.88	0.48	0.48	0.99	0.00	1.88	1.43	1.50	1.50	0.34
		(1.50	0.08	0.06	0.06	0.90	0.48	0.48	0.99	0.01	1.88	1.47	1.49	1.49	0.41)
$1^2\Gamma$	$0.67\lvert 1\sigma^2 2\sigma^2 3\sigma^1 1\pi_x^2 1\pi_y^2(1\delta_+^2 - 1\delta_-^2)\rangle$	0.94	0.14	0.01	0.01	0.62	0.37	0.37	1.00	1.00	1.89	1.39	1.59	1.59	0.50
		(0.93	0.12	0.01	0.01	0.62	0.38	0.38	0.99	0.99	1.89	1.41	1.57	1.57	0.52)
$A^4\Pi$	$0.66\lvert 1\sigma^2 2\sigma^2 3\sigma^1 1\pi_x^2 1\pi_y^2(2\pi_x^1 1\delta_+^1 + 2\pi_y^1 1\delta_-^1)\rangle$	0.89	0.09	0.05	0.05	0.64	0.79	0.82	0.52	0.52	1.91	1.43	1.61	1.61	0.59
		(0.85	0.08	0.06	0.07	0.64	0.78	0.81	0.53	0.52	1.91	1.44	1.60	1.60	0.62)
$1^2\Sigma^+$	$0.67\lvert 1\sigma^2 2\sigma^2 3\sigma^1 1\pi_x^2 1\pi_y^2(1\delta_+^2 + 1\delta_-^2)\rangle$	0.95	0.06	0.01	0.01	0.69	0.39	0.39	0.96	0.96	1.88	1.41	1.61	1.61	0.56
		(0.92	0.08	0.02	0.02	0.67	0.41	0.41	0.92	0.97	1.90	1.42	1.58	1.58	0.54)
$B^4\Pi$	$0.93\lvert 1\sigma^2 2\sigma^2 1\pi_x^2 1\pi_y^2 2\pi_y^1 1\delta_+^1 1\delta_-^1\rangle$	0.14	0.02	0.05	0.11	0.45	0.31	1.05	0.98	0.98	1.93	1.47	1.63	1.78	0.85
		(0.13	0.02	0.04	0.16	0.47	0.39	1.01	0.96	0.96	1.94	1.47	1.56	1.75	0.79)
$1^2\Phi$	$0.57\lvert 1\sigma^2 2\sigma^2 3\sigma^1 1\pi_x^2 1\pi_y^2(\overline{2\pi_y^1 1\delta_-^1} + 2\pi_x^1\overline{1\delta_+^1})\rangle +$	0.98	0.14	0.03	0.03	0.60	0.82	0.82	0.51	0.51	1.88	1.37	1.62	1.62	0.54
	$0.33\lvert 1\sigma^2 2\sigma^2 3\sigma^1 1\pi_x^2 1\pi_y^2(2\pi_y^1\overline{1\delta_-^1} + \overline{2\pi_x^1 1\delta_+^1})\rangle$	(0.97	0.12	0.04	0.04	0.61	0.80	0.80	0.50	0.50	1.89	1.38	1.62	1.62	0.57)

VO correlates *diabatically* to the first excited state of $V^+(^5F) + O^-(^2P)$. The valence-bond-Lewis diagram (1) captures the essence of bonding, suggesting a triple bond (σ, π_x, π_y) between V^+ and O^-. The Mulliken analysis indicates a flow of 0.80 e^- through the π system from O^- to V^+, partially neutralized by a counter flow of 0.30 e^- through the σ frame, leaving the in situ V atom with a charge of about +0.5.

From Table 5 we infer that in all correlated levels from MRCI/B down to C-RCCSD(T)+DKH2/BP, our numerical values are in good to excellent agreement with experimental

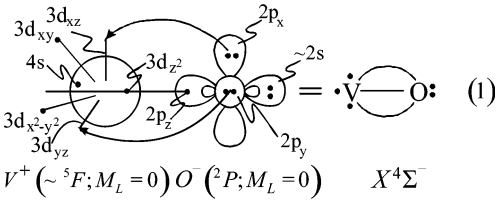

(1)

results. At the highest level of theory C-MRCI+DKH2+Q/BP and C-RCCSD(T)+DKH2/BP the binding energies and bond distances are $D_e = 151.7$, 149.2 kcal/mol and $r_e = 1.591$, 1.583 Å, respectively, as contrasted to an experimental bond distance of 1.589 Å.[4] Correcting the D_e for zero point energy (ZPE) and BSSE we obtain $D_0 = 149.8$ kcal/mol at the C-MRCI+DKH2+Q/BP level, in excellent agreement with experiment. Note that relativistic effects play only a minor role, reducing for instance the binding energy by less than 1 kcal/mol. It is interesting to obtain the D_0 at the C-MRCI+Q/B level of theory: $D_0 = D_e - \text{ZPE} - \text{BSSE} = 155.0 - 1.42 - 3.39 = 150.2$ kcal/mol at $r_e = 1.594$ Å, also in very good agreement with experiment.

Observe the significant differences in the dipole moment between expectation ($\langle\mu\rangle$) and finite field (μ_{FF}) values at the configuration interaction level; μ_{FF} is always larger than $\langle\mu\rangle$.[46] The agreement of μ_{FF} values with experiment[14] is very good at all correlated levels of theory and indeed excellent at the RCCSD(T)/B down to C-RCCSD(T)+DKH2/BP; Table 5.

$a^2\Sigma^-$, $1^2\Delta$, $1^2\Gamma$, $1^2\Sigma^+$, $1^2\Phi$. With the exception of the $1^2\Delta$ state whose bonding character is not very clear (see below), the $a^2\Sigma^-$, $1^2\Phi$ and $1^2\Gamma$, $1^2\Sigma^+$ doublets can be considered as ionic (Table 6), correlating *diabatically* to the second and eighth excited states of V^+, $^3F(4s^13d^3)$ and $b^3G(4s^13d^3)$, 0.742 and 1.702 eV,[45] respectively, above its first excited state $^5F(4s^13d^3)$; see Table 4.

$a^2\Sigma^-$ is the first excited state of VO located (experimentally)[15] 5630 ± 80 cm^{-1} above the ground state, correlating diabatically to $V^+(^3F;M_L{=}0) + O^-(^2P;M_L{=}0)$. The $|^3F;M_L{=}0\rangle$ vector of V^+ is described by the linear combination

$$|^3F;M_L{=}0\rangle_{A_2} = 0.73|4s^1\overline{3d^1_{x^2-y^2}}3d^1_{xy}3d^1_{z^2}\rangle + 0.42|4s^13d^1_{x^2-y^2}3d^1_{xy}\overline{3d^1_{z^2}}\rangle + 0.36|4s^13d^1_{x^2-y^2}3d^1_{xz}3d^1_{yz}\overline{3d^1_{z^2}}\rangle + 0.30|4s^13d^1_{x^2-y^2}\overline{3d^1_{xy}}3d^1_{z^2}\rangle + 0.21|4s^1\overline{3d^1_{xz}}3d^1_{yz}3d^1_{z^2}\rangle + 0.15|4s^13d^1_{xz}\overline{3d^1_{yz}}3d^1_{z^2}\rangle$$

Only the "0.73" and "0.30" components are conducive to bonding with the $O^-(^2P)$ in the $M_L = 0$ orientation, and this is reflected to the two leading configurations of the $a^2\Sigma^-$ state shown in Table 6: The coefficients "0.81" and "0.47" trace the "0.73" and "0.30" ones in the $|^3F;M_L{=}0\rangle$ expansion of V^+. Taking into account the population analysis, the bonding of the $a^2\Sigma^-$ state can be represented by the vbL diagram (1), but with the spins of the $3d^1_{x^2-y^2}(\delta_+)$, $3d^1_{xy}(\delta_-)$ spectator electrons coupled into a singlet. The bonding similarity of the $a^2\Sigma^-$ and $X^4\Sigma^-$ states is further corroborated by the fact that their (diabatic) calculated dissociation energies with respect to $V^+(^3F)$ and $V^+(^5F)$, respectively, are the same, because of equal energy splittings of $V^+(^3F)-V^+(^5F)$ and $a^2\Sigma^- - X^4\Sigma^-$; Tables 4 and 5. The experimentally determined $\Delta G_{1/2}$ and T_o values are in relative agreement with the calculated ones at all levels of theory.

Experimental D_0 values can be obtained for all states studied, except $1^2\Gamma$, by subtracting the experimental separation energies T_o from the D_0 of the $X^4\Sigma^-$ state, because all states examined correlate *adiabatically* to the same end products. Therefore, $D_0(a^2\Sigma^-) = D_0(X^4\Sigma^-) - T_o(a^2\Sigma^- \leftarrow X^4\Sigma^-) = 149.5 \pm 2$ kcal/mol $- 5630 \pm 80$ cm^{-1} $= 133.4 \pm 2.2$ kcal/mol, in agreement with the C-MRCI+DKH2+Q/BP $D_0 = D_e - \text{ZPE} - \text{BSSE} = 134.4 - 1.9 = 132.5$ kcal/mol.

From the states studied $1^2\Delta$ seems to be the less ionic, featuring a total Mulliken charge transfer from V to O of about 0.3 e$^-$. The bonding comprises two π bonds and a σ interaction. The C-MRCI or C-MRCI+DKH2/BP r_e values are in excellent agreement with experiment and the same is true for the C-MRCI+DKH2+Q/BP $D_0 = D_e - \text{ZPE} - \text{BSSE} = 126.1 - 1.9 = 124.2$ kcal/mol.

In ascending order the next two doublets are of $1^2\Gamma$ and $1^2\Sigma^+$ symmetry, the former never observed experimentally and calculated here for the first time. At the highest level of calculation C-MRCI+DKH2+Q/BP the $T_e(1^2\Sigma^+ \leftarrow X^4\Sigma^-)$ value is in good agreement with experiment,[13] whereas a $T_e(1^2\Gamma \leftarrow X^4\Sigma^-)$ value of 9000 cm^{-1} is recommended for the $1^2\Gamma$ state obtained at the same level of theory (Table 5). Note as well the excellent agreement between experiment and theory of the r_e value of the $1^2\Sigma^+$ state.

The atomic populations on the metal ($4s^13d^3$) coupled with the ionic bonding character of these two states suggest that their diabatic end products should be $V^+(b^3G(4s^13d^3)) + O^-(^2P)$; the V^+ b^3G term is located 16 446.05 cm^{-1} (=2.039 eV)[45] above the V^+ ground state. The $M_L = 0$ and ± 4 components of the b^3G vector are

$$|b^3G;M_L{=}0\rangle_{A_1} = 0.38|4s^13d^1_{z^2}(3d^2_{xy} + 3d^2_{x^2-y^2})\rangle + 0.33|4s^13d^1_{x^2-y^2}(3d^2_{xz} - 3d^2_{yz})\rangle + 0.40|4s^13d^1_{xz}\overline{3d^1_{yz}}3d^1_{xy}\rangle - 0.23|4s^1\overline{3d^1_{xz}}3d^1_{yz}3d^1_{xy}\rangle + 0.38|4s^13d^1_{z^2}(3d^2_{xz} + 3d^2_{yz})\rangle$$

$$|b^3G;M_L{=}\pm4\rangle_{A_1} = 0.45|4s^13d^1_{z^2}(3d^2_{xy} - 3d^2_{x^2-y^2})\rangle + 0.34|4s^13d^1_{x^2-y^2}(3d^2_{yz} - 3d^2_{xz})\rangle + 0.47|4s^13d^1_{xz}\overline{3d^1_{yz}}3d^1_{xy}\rangle - 0.27|4s^1\overline{3d^1_{xz}}3d^1_{yz}3d^1_{xy}\rangle$$

Combined with the $^2P(M_L{=}0)$ term of the O^- anion the above vectors give rise to the $1^2\Gamma$ and $1^2\Sigma^+$ states of VO, respectively. Only the $|4s^13d^1_{z^2}(3d^2_{xy} - 3d^2_{x^2-y^2})\rangle$ parts of the $M_L = 0, \pm4$ components are best suited for bonding with the $M_L = 0$ orientation of the O^- ^2P vector due to the absence of d_{xy}, d_{yz} repulsive distributions. The bonding of the $1^2\Gamma$ and $1^2\Sigma^+$ states is shown graphically in the vbL diagram (2). About 0.8 e$^-$ are

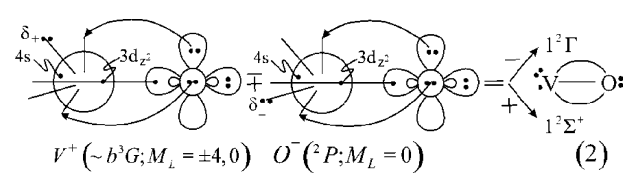

(2)

transferred from O^- to V^+ through the π system and 0.3 e$^-$ through the σ in opposite direction, resulting to a (π_x, π_y, σ) triple bond.

The highest calculated state is of $^2\Phi$ symmetry located (experimentally) $14\,920 \pm 90$ cm^{-1} above the $X^4\Sigma^-$ state; the $1^2\Phi \leftarrow X^4\Sigma^-$ energy separation compares favorably with all our calculated C-MRCI numbers. In addition, the experimental bond distance is in excellent agreement with the calculated ones after core-valence correlation is taken into account in the MRCI

calculations. Diabatically it correlates to $V^+(^3F;M_L=\pm2$ or $\pm3) + O^-(^2P;M_L=\pm1$ or 0), featuring a double (σ, π) bond.

$A'^4\Phi$, $A^4\Pi$, $B^4\Pi$. The A′, A quartets (experimental notation) correlate diabatically to the first excited state of V^+, $^5F(4s^1\text{-}3d^3;M_L=\pm2) = |4s^1 3d^1_{xz} 3d^1_{yz} 3d^1_{xy}\rangle$ and $O^-(^2P;M_L=\pm1,\mp1)$. Their bonding character (σ, π) is shown graphically in the vbL diagram (3). About 0.3 e^- are moving from the V^+ ion to the

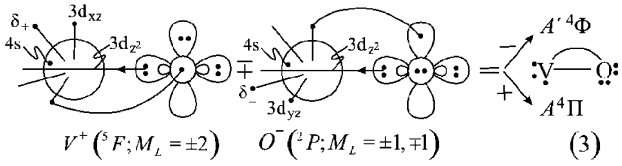

O^- through the π-system, and 0.7 e^- are transferred via the σ system filling the empty d_{z^2} (d_σ) orbital. The 4s and d_δ electrons being localized on the metal ion do not play any significant role in the bonding. All our calculated results for both A′, A quartets are in very good agreement with the experiment. See Table 5.

$B^4\Pi$ is the most ionic of all states studied with a Mulliken charge transfer of approximately 0.8 e^- from V to O atom. This is also reflected in the very high dipole moment of this state, $\mu \approx 6.5-7$ Debye. It is interesting that this is the only state that correlates *diabatically* to the ground state cation, $V^+(^5D,d^4,M_L=0) + O^-(^2P;M_L=\pm1)$, described satisfactorily by a single configuration; Table 6. The bonding is presented clearly in the following diagram, suggesting a σ and a π bond. Our calculated

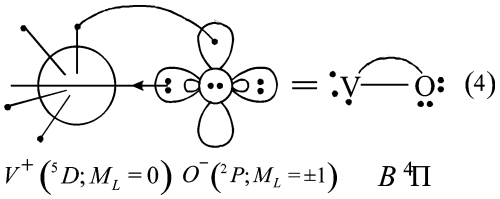

numbers can be considered in good agreement with the experimental findings.

B. VO^+. From the first three states of $V^+(^5D,^5F,^3F) + O(^3P)$ one can obtain molecular VO^+ states of multiplicities 7, 5, 3, and 1. We have calculated a total of 11 states, five singlets ($^1\Gamma$, $^1\Sigma^+$, $^1\Delta$, $^1\Pi$, $^1\Phi$), four triplets ($X^3\Sigma^-$, $^3\Phi$, $^3\Delta$, $^3\Pi$), and two quintets ($^5\Pi$, $^5\Sigma^-$) whose potential energy curves are shown in Figure 2. The triplets and the quintets correlate *adiabatically* to $V^+(^5D) + O(^3P)$, whereas the five singlets to $V^+(^3F) + O(^3P)$. Published theoretical results for the ground state of VO^+ ($X^3\Sigma^-$) are listed in Table 2; four excited states ($^3\Delta$, $^1\Delta$, $^5\Pi$, $^5\Sigma^-$) have also been studied by DFT methods.[31,32]

On the basis of Mulliken atomic electron densities (Table 8), the equilibrium structure of the states studied can be interpreted as ionic, i.e., $V^{2+}O^-$. Under this premise the triplets and quintets correlate *diabatically* to the ground state of $V^{2+}(a^4F;3d^3)$, and the singlets to the first doublet of $V^{2+}(a^2G;3d^3)$ 11 517 cm^{-1} above the a^4F.[45] We describe first the triplets, then the singlets followed by the two quintets.

$X^3\Sigma^-$, $^3\Delta$, $^3\Phi$, $^3\Pi$. The $X^3\Sigma^-$ configuration function and its Mulliken population analysis are indicative to an in situ $V^{2+}(^4F;M_L=0) + O^-(^2P;M_L=0)$ character, or that the bonding is described fairly well by the vbL diagram (1) after removing the 4s (3σ) electron localized on the $V^+(\sim^5F)$ atom. About 0.9 e^- are moving from O^- to V^{2+} through the π-system, whereas 0.3 e^- are transferred in the opposite direction through the σ route, leaving the in situ V atom with a charge of +1.4 e^-. At the highest level of calculation C-MRCI+DKH2+Q/BP (or

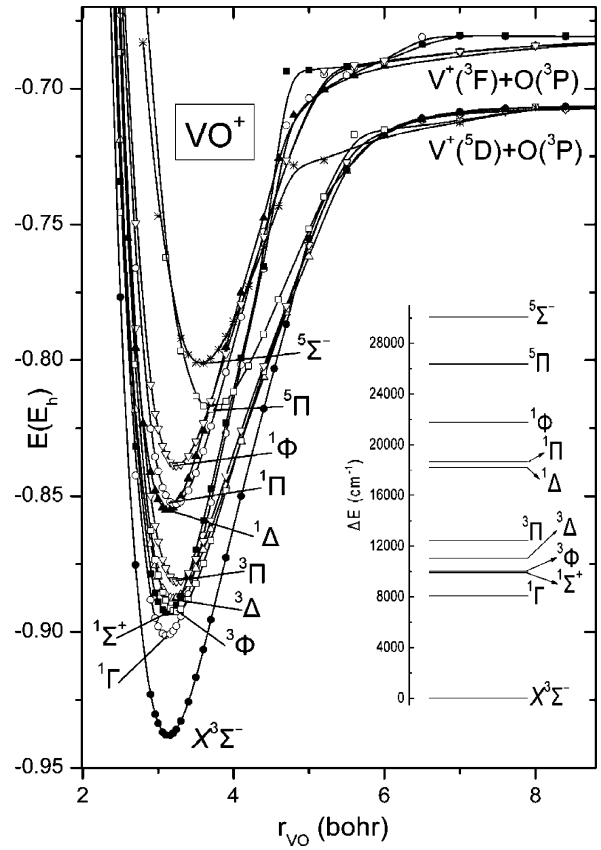

Figure 2. MRCI+Q potential energy curves and energy levels (inset) of VO^+. All energies are shifted by +1017.0 hartree.

C-RCCSD(T)+DKH2/BP) the dissociation energy is in excellent agreement with the experimental results; the same holds true for the internuclear distance r_e. Finally, the experimental ionization energy[26] IE = 7.25 ± 0.01 eV compares very favorably with the C-MRCI+DKH2+Q/BP (C-RCCSD(T)+DKH2/BP) IE = 7.33 (7.24) eV.

The removal of one electron from the $4s^2$ ($3\sigma^2$) orbital of the VO $1^2\Delta$ state gives rise to the $^3\Delta$ state of VO^+, located (experimentally) 9437 ± 161 cm^{-1} above the $X^3\Sigma^-$ state; Table 7. Similarly to the $1^2\Delta$ state of the neutral, a triple bond character can be discerned with a total charge transfer of about 0.3 e^- from V^+ to the oxygen atom. At the C-MRCI+DKH2+Q/BP (C-RCCSD(T)+DKH2/BP) a T_e = 9622 (9634) cm^{-1} is obtained, in agreement with the experimental findings. Notice that the inclusion of relativistic effects is here crucial in bringing the calculated T_e value in agreement with the experimental one.

There are no experimental results for the $^3\Phi$ and $^3\Pi$ states. Ionization of the $A'^4\Phi$ and $A^4\Pi$ states of the neutral VO, i.e., detachment of the $4s^1$ ($3\sigma^1$) electron, results in the $^3\Phi$ and $^3\Pi$ states, respectively; see the vbL diagram (3). For both states their *diabatic* end products can be considered to be $V^{2+}(^4F;M_L=\pm2) + O^-(^2P;M_L=\pm1,\mp1)$ in complete analogy with the bonding diagram (3).

$^1\Gamma$, $^1\Sigma^+$, $^1\Delta$, $^1\Pi$, $^1\Phi$. $^1\Gamma$ is the first excited state of VO^+, about 7500 cm^{-1} above the $X^3\Sigma^-$ state (Table 7), followed by the $^1\Sigma^+$ state. The latter is practically degenerate with the $^3\Phi$ and $^3\Delta$ states of VO^+ (Figure 2); however, at all levels of theory it is consistently lower than the $^3\Phi$ state. Note that the $^1\Gamma$ has not been explored before either experimentally or theoretically. Perhaps, one would expect that the first excited state should be of $^1\Sigma^-$ symmetry, tracing the first excited state of VO ($a^2\Sigma^-$) after removing the $4s^1$ ($3\sigma^1$) electron from the metal. Neverthe-

TABLE 7: Total Energies E (hartree), Equilibrium Bond Distances r_e (Å), Dissociation Energies D_e (kcal/mol), Harmonic Frequencies ω_e and Anharmonicities $\omega_e x_e$ (cm^{-1}), Rotational−Vibrational Constants a_e (10^{-3} cm^{-1}), and Energy Separations T_e (cm^{-1}) of VO^+

method[a]	$-E$	r_e	D_e[b]	ω_e	$\omega_e x_e$	a_e	T_e
			$X^3\Sigma^-$				
CASSCF/B	1017.68073	1.560	125.0	1083	5.0	3.3	0.0
MRCI/B	1017.92365	1.564	143.4	1055	5.3	3.5	0.0
MRCI+Q/B	1017.93758	1.567	145.5	1045	5.6	3.6	0.0
MRCI/BP	1017.92479	1.562	142.8	1053	5.3	3.5	0.0
MRCI+Q/BP	1017.93875	1.566	144.7	1043	5.3	3.4	0.0
C-MRCI/B	1018.22400	1.554	137.9	1056	5.2	3.5	0.0
C-MRCI+Q/B	1018.27329	1.558	140.2	1049	5.2	3.5	0.0
C-MRCI/BP	1018.28251	1.554	135.6	1058	5.2	3.6	0.0
C-MRCI+Q/BP	1018.33635	1.558	137.7	1052	4.7	3.5	0.0
C-MRCI+DKH2/BP	1023.57921	1.553	136.1	1069	5.2	3.9	0.0
C-MRCI+DKH2+Q/BP	1023.63298	1.557	137.9	1056	4.9	3.6	0.0
RCCSD(T)/B	1017.93602	1.562	133.5	1082	7.2	3.7	0.0
C-RCCSD(T)/B	1018.27864	1.551	137.4				0.0
C-RCCSD(T)/BP	1018.34392	1.550	134.4	1097	5.3	3.4	0.0
C-RCCSD(T)+DKH2/BP	1023.64190	1.549	137.9				0.0
expt		1.54 ± 0.01[c]	137.9 ± 2.3[c] 138.1 ± 2.3[e]	1053 ± 5[d]			0.0
			$^1\Gamma$				
CASSCF/B	1017.64368	1.551	120.1	1111	4.3	3.1	8132
MRCI/B	1017.88682	1.554	137.2	1088	4.9	3.3	8083
MRCI+Q/B	1017.90072	1.557	138.1	1078	4.8	3.3	8089
C-MRCI/B	1018.18925	1.545	144.4	1089	4.9	3.6	7626
C-MRCI+Q/B	1018.23877	1.548	146.9	1085	4.4	2.8	7576
C-MRCI/BP	1018.24866	1.545	142.7	1094	4.8	3.3	7429
C-MRCI+Q/BP	1018.30282	1.549	145.3	1091	4.3	2.9	7360
C-MRCI+DKH2/BP	1023.54576	1.544	141.6	1097	4.7	3.6	7343
C-MRCI+DKH2+Q/BP	1023.59985	1.547	144.1	1099	4.9	3.3	7270
			$^1\Sigma^+$				
CASSCF/B	1017.61885	1.555	105.4	1092	5.2	3.2	13581
MRCI/B	1017.87565	1.559	130.1	1069	5.3	3.4	10534
MRCI+Q/B	1017.89233	1.563	132.8	1059	5.4	3.5	9931
C-MRCI/B	1018.17518	1.549	135.6	1071	5.3	3.3	10714
C-MRCI+Q/B	1018.22878	1.553	140.7	1068	5.4	3.4	9767
C-MRCI/BP	1018.23412	1.549	133.5	1073	5.2	3.3	10621
C-MRCI+Q/BP	1018.29236	1.553	138.6	1076	5.3	3.3	9656
C-MRCI+DKH2/BP	1023.53129	1.548	132.6	1077	5.7	3.7	10518
C-MRCI+DKH2+Q/BP	1023.58951	1.552	137.7	1079	6.2	4.1	9540
			$^3\Phi$				
CASSCF/B	1017.60240	1.642	75.9	905	6.2	3.9	17191
MRCI/B	1017.87204	1.621	103.1	955	5.9	3.8	11326
MRCI+Q/B	1017.89185	1.618	107.7	962	6.3	3.7	10036
C-MRCI/B	1018.16747	1.614	102.6	962	6.2	3.7	12408
C-MRCI+Q/B	1018.22460	1.610	109.8	967	6.3	3.6	10685
C-MRCI/BP	1018.22637	1.612	100.1	968	6.6	3.7	12322
C-MRCI+Q/BP	1018.28723	1.609	106.5	972	6.4	3.5	10782
C-MRCI+DKH2/BP	1023.52292	1.610	101.0	972	6.5	3.8	12354
C-MRCI+DKH2+Q/BP	1023.58383	1.608	107.2	983	6.6	3.6	10787
			$^3\Delta$				
CASSCF/B	1017.62708	1.576	91.3	938	6.1	4.8	11774
MRCI/B	1017.87246	1.595	103.3	911	5.6	4.3	11234
MRCI+Q/B	1017.88714	1.600	104.7	898	5.7	4.3	11069
C-MRCI/B	1018.17389	1.581	106.5	908	5.4	4.3	10998
C-MRCI+Q/B	1018.22529	1.587	110.0	904	5.5	4.3	10533
C-MRCI/BP	1018.23159	1.583	104.5	905	5.3	4.4	11175
C-MRCI+Q/BP	1018.28704	1.591	107.0	910	5.4	4.3	10823
C-MRCI+DKH2/BP	1023.53398	1.581	108.2	912	5.6	4.4	9928
C-MRCI+DKH2+Q/BP	1023.58914	1.588	110.7	915	4.8	4.4	9622
RCCSD(T)/B	1017.88625	1.590	102.4				10925
C-RCCSD(T)/B	1018.22965	1.574	106.8				10752
C-RCCSD(T)/BP	1018.29437	1.573	103.5	925	4.5	5.0	10874
C-RCCSD(T)+DKH2/BP	1023.59800	1.565	110.5	928	4.4	5.1	9634
expt[f]							9437 ± 161
			$^3\Pi$				
CASSCF/B	1017.59264	1.656	69.9	859	7.0	4.3	19334
MRCI/B	1017.86165	1.631	96.6	919	6.4	4.0	13607
MRCI+Q/B	1017.88090	1.628	100.8	926	6.4	4.0	12440
C-MRCI/B	1018.15784	1.622	96.6	921	6.2	4.3	14521
C-MRCI+Q/B	1018.21470	1.617	103.5	927	6.6	3.9	12857
C-MRCI/BP	1018.21597	1.621	93.9	924	5.9	4.5	14603
C-MRCI+Q/BP	1018.27711	1.617	100.3	929	6.7	3.7	13002
C-MRCI+DKH2/BP	1023.51247	1.619	94.3	935	5.8	3.9	14647
C-MRCI+DKH2+Q/BP	1023.57367	1.615	100.8	929	6.5	3.7	13018

TABLE 7: Continued

method[a]	$-E$	r_e	D_e[b]	ω_e	$\omega_e x_e$	a_e	T_e
			$^1\Delta$				
CASSCF/B	1017.58112	1.548	81.6	1052	6.6	4.6	21862
MRCI/B	1017.83761	1.562	106.5	1022	4.7	3.1	18883
MRCI+Q/B	1017.85463	1.566	109.5	1011	5.5	3.8	18206
C-MRCI/B	1018.13879	1.554	112.8	1040	6.0	3.9	18702
C-MRCI+Q/B	1018.19427	1.559	119.0	1042	5.8	3.6	17343
C-MRCI/BP	1018.19714	1.553	110.7	1037	5.8	3.8	18736
C-MRCI+Q/BP	1018.25761	1.558	116.9	1039	5.6	3.7	17282
C-MRCI+DKH2/BP	1023.50010	1.552	113.2	1045	7.2	3.6	17362
C-MRCI+DKH2+Q/BP	1023.56056	1.557	119.2	1043	6.3	4.0	15895
			$^1\Pi$				
CASSCF/B	1017.55728	1.635	63.7	935	4.9	3.5	27094
MRCI/B	1017.83230	1.614	102.2	963	5.0	3.5	20049
MRCI+Q/B	1017.85261	1.612	107.4	971	5.1	3.5	18649
C-MRCI/B	1018.13030	1.607	107.3	981	6.8	3.7	20565
C-MRCI+Q/B	1018.18927	1.605	115.8	983	5.5	3.5	18440
C-MRCI/BP	1018.18901	1.608	105.2	979	6.8	3.7	20521
C-MRCI+Q/BP	1018.25265	1.606	113.7	981	5.6	3.6	18370
C-MRCI+DKH2/BP	1023.48669	1.607	104.8	989	10.7	4.1	20306
C-MRCI+DKH2+Q/BP	1023.55049	1.604	112.9	990	8.0	3.9	18105
			$^1\Phi$				
CASSCF/B	1017.54843	1.651	58.4	882	4.9	3.7	29036
MRCI/B	1017.81896	1.626	93.9	922	5.3	3.8	22977
MRCI+Q/B	1017.83846	1.623	98.7	924	5.5	3.8	21754
C-MRCI/B	1018.11778	1.619	99.5	936	6.4	3.9	23313
C-MRCI+Q/B	1018.17544	1.615	107.1	939	6.4	3.8	21476
C-MRCI/BP	1018.17680	1.620	97.6	932	5.1	3.7	23201
C-MRCI+Q/BP	1018.23919	1.618	105.2	937	5.6	3.6	21324
C-MRCI+DKH2/BP	1023.47447	1.618	97.1	937	6.6	3.9	22988
C-MRCI+DKH2+Q/BP	1023.53695	1.616	104.4	942	8.1	4.2	21076
			$^5\Pi$				
CASSCF/B	1017.58773	1.904	66.6	650	2.6	2.3	20411
MRCI/B	1017.80399	1.859	60.4	671	2.8	2.1	26261
MRCI+Q/B	1017.81745	1.855	61.1	671	2.7	2.1	26365
C-MRCI/B	1018.09868	1.842	59.5	682	2.9	2.2	27505
C-MRCI+Q/B	1018.14514	1.830	60.0	687	3.0	2.4	28124
C-MRCI/BP	1018.15772	1.843	57.2	680	3.1	2.5	27389
C-MRCI+Q/BP	1018.20852	1.831	57.4	685	2.6	2.1	28056
C-MRCI+DKH2/BP	1023.45668	1.832	59.3	685	3.2	2.0	26892
C-MRCI+DKH2+Q/BP	1023.50745	1.824	59.0	689	3.3	2.6	27550
RCCSD(T)/B	1017.81851	1.859	59.7				25792
C-RCCSD(T)/B	1018.15557	1.830	60.2	680			27011
C-RCCSD(T)/BP	1018.22141	1.831	57.7	689	1.8	1.5	26887
C-RCCSD(T)+DKH2/BP	1023.52053	1.823	61.8	693	2.5	1.8	26637
expt[g]							26858 ± 242
			$^5\Sigma^-$				
CASSCF/B	1017.56620	1.818	53.3	718	3.5	2.3	25137
MRCI/B	1017.78606	1.783	49.1	745	6.7	3.9	30196
MRCI+Q/B	1017.80048	1.781	50.5	742	6.3	3.7	30090
C-MRCI/B	1018.08141	1.763	48.7	752	5.8	3.8	31295
C-MRCI+Q/B	1018.12895	1.754	49.8	755	5.5	3.9	31679
C-MRCI/BP	1018.14006	1.764	46.1	750	6.0	3.7	31265
C-MRCI+Q/BP	1018.19194	1.755	47.0	753	5.8	3.9	31694
C-MRCI+DKH2/BP	1023.43804	1.757	47.5	758	6.1	3.9	30983
C-MRCI+DKH2+Q/BP	1023.48991	1.747	48.2	760	6.2	4.0	31400
RCCSD(T)/B	1017.80117	1.781	48.9	731	2.9	2.3	29597
C-RCCSD(T)/B	1018.13974	1.753	50.3	754	3.7	2.5	30486
C-RCCSD(T)/BP	1018.20524	1.754	47.5	751	3.6	2.5	30436
C-RCCSD(T)+DKH2/BP	1023.50337	1.745	51.0	755	3.7	2.3	30403
expt[g]							30730 ± 242

[a] Internally contracted MRCI and C-MRCI calculations. +Q and DKH2 refer to the Davidson correction and to second order Douglas–Kroll–Hess relativistic corrections. B and BP refer to Bauschlicher and Balabanov–Petterson basis sets on V; see text. [b] With respect to the adiabatic fragments of each state, i.e., singlet states correlate to $V^+(^3F) + O(^3P)$, and both triplets and quintets correlate to $V^+(^5D) + O(^3P)$. [c] Reference 26. [d] Reference 29. [e] Reference 28. [f] "Experimental" T_e value obtained using the relation $T_e(^3\Delta) = IE(VO(X^4\Sigma^-)\rightarrow VO^+(^3\Delta)) - IE(VO(X^4\Sigma^-)\rightarrow VO^+(X^3\Sigma^-)) = (8.42 \pm 0.01\ eV)^{26} - (7.25 \pm 0.01\ eV)^{26} = 9437 \pm 161\ cm^{-1}$. [g] These T_e values were obtained through a similar relation with that of footnote *f*. $T_e(^5\Pi) = (10.58 \pm 0.02\ eV)^{26} - (7.25 \pm 0.01\ eV)^{26} = 26858 \pm 242\ cm^{-1}$ and $T_e(^5\Sigma^-) = (11.06 \pm 0.02\ eV)^{26} - (7.25 \pm 0.01\ eV)^{26} = 30730 \pm 242\ cm^{-1}$. The bands at 10.58 ± 0.02 and 11.06 ± 0.02 eV are characterized as subsidiary maxima of a broad band at 11.41 ± 0.02 eV by the authors of ref 26.

less, this is not the case and it seems that the $^1\Gamma$ of VO^+ correlates *diabatically* to $V^{2+}(a^2G;M_L=\pm4) + O^-(^2P;M_L=0)$. We can think of the $^1\Gamma$ as resulting from the $1^2\Gamma$ state of VO by removing the $4s^1$ ($3\sigma^1$) electron of the V^+

TABLE 8: Dominant Equilibrium CASSCF Configurations, CASSCF and MRCI (in Parentheses) Mulliken Atomic Populations, and Total Charge (q_v) on the Vanadium Atom of the VO^+ Species[a]

		populations													
		V									O				
state	configurations	4s	$4p_z$	$4p_x$	$4p_y$	$3d_{z^2}$	$3d_{xz}$	$3d_{yz}$	$3d_{x^2-y^2}$	$3d_{xy}$	2s	$2p_z$	$2p_x$	$2p_y$	q_v
$X^3\Sigma^-$	$0.94\|1\sigma^2 2\sigma^2 1\pi_x^2 1\pi_y^2 1\delta_+^1 1\delta_-^1\rangle$	0.02	0.01	0.00	0.00	0.67	0.43	0.43	1.00	1.00	1.93	1.35	1.54	1.54	1.42
		(0.03	0.02	0.01	0.01	0.64	0.39	0.39	0.98	0.98	1.90	1.42	1.57	1.57	1.42)
$^1\Gamma$	$0.67\|1\sigma^2 2\sigma^2 1\pi_x^2 1\pi_y^2 (1\delta_+^2 - 1\delta_-^2)\rangle$	0.02	0.01	0.02	0.02	0.68	0.43	0.43	1.00	1.00	1.93	1.35	1.54	1.54	1.43
		(0.02	0.01	0.00	0.00	0.67	0.43	0.43	0.99	0.99	1.91	1.35	1.53	1.53	1.42)
$^1\Sigma^+$	$0.67\|1\sigma^2 2\sigma^2 1\pi_x^2 1\pi_y^2 (1\delta_+^2 + 1\delta_-^2)\rangle$	0.02	0.01	0.00	0.00	0.68	0.43	0.43	0.99	0.99	1.93	1.35	1.54	1.54	1.42
		(0.03	0.01	0.00	0.00	0.67	0.44	0.44	0.97	0.97	1.92	1.35	1.53	1.53	1.42)
$^3\Delta$	$0.92\|1\sigma^2 2\sigma^2 3\sigma^1 1\pi_x^2 1\pi_y^2 1\delta_+^1\rangle$	0.61	0.00	0.00	0.00	0.99	0.54	0.54	1.00	0.01	1.88	1.50	1.43	1.43	1.29
		(0.60	0.01	0.00	0.00	0.98	0.54	0.54	1.00	0.01	1.87	1.50	1.42	1.42	1.30)
$^3\Phi$	$0.63\|1\sigma^2 2\sigma^2 1\pi_x^2 1\pi_y^2 (2\pi_x^1 1\delta_+^1 - 2\pi_y^1 1\delta_-^1)\rangle$	0.03	0.01	0.01	0.01	0.64	0.90	0.90	0.50	0.50	1.94	1.36	1.57	1.57	1.50
		(0.03	0.02	0.01	0.01	0.64	0.88	0.88	0.50	0.50	1.92	1.35	1.56	1.56	1.49)
$^3\Pi$	$0.63\|1\sigma^2 2\sigma^2 1\pi_x^2 1\pi_y^2 (2\pi_x^1 1\delta_+^1 + 2\pi_y^1 1\delta_-^1)\rangle$	0.03	0.01	0.00	0.00	0.61	0.91	0.91	0.49	0.51	1.94	1.38	1.56	1.56	1.49
		(0.04	0.02	0.01	0.01	0.62	0.89	0.89	0.50	0.50	1.92	1.37	1.55	1.55	1.48)
$^1\Delta$	$0.93\|1\sigma^2 2\sigma^2 3\sigma^1 1\pi_x^2 1\pi_y^2 \overline{1\delta_+^1}\rangle$	0.71	0.00	0.00	0.00	1.02	0.49	0.49	1.00	0.01	1.87	1.37	1.47	1.47	1.25
		(0.72	0.01	0.00	0.00	0.99	0.50	0.50	0.99	0.01	1.86	1.37	1.46	1.46	1.24)
$^1\Pi$	$0.63\|1\sigma^2 2\sigma^2 1\pi_x^2 1\pi_y^2 (\overline{2\pi_x^1} 1\delta_+^1 + 2\pi_y^1 \overline{1\delta_-^1})\rangle$	0.04	0.01	0.00	0.00	0.60	0.93	0.93	0.50	0.50	1.94	1.39	1.54	1.54	1.46
		(0.04	0.02	0.01	0.01	0.61	0.90	0.90	0.50	0.50	1.92	1.38	1.54	1.54	1.46)
$^1\Phi$	$0.63\|1\sigma^2 2\sigma^2 1\pi_x^2 1\pi_y^2 (\overline{2\pi_x^1} 1\delta_+^1 - 2\pi_y^1 \overline{1\delta_-^{-1}})\rangle$	0.04	0.01	0.00	0.00	0.56	0.92	0.92	0.54	0.54	1.94	1.43	1.51	1.51	1.44
		(0.04	0.02	0.01	0.01	0.57	0.89	0.89	0.54	0.54	1.92	1.42	1.51	1.51	1.44)
$^5\Pi$	$0.98\|1\sigma^2 2\sigma^2 3\sigma^1 1\pi_x^2 1\pi_y^1 1\delta_+^1 1\delta_-^1\rangle$	0.20	0.06	0.03	0.01	1.03	0.13	0.06	1.00	1.00	1.95	1.74	1.81	0.92	1.45
		(0.21	0.05	0.03	0.01	1.03	0.18	0.06	0.99	0.99	1.94	1.72	1.76	0.93	1.41)
$^5\Sigma^-$	$0.98\|1\sigma^2 2\sigma^1 3\sigma^1 1\pi_x^2 1\pi_y^2 1\delta_+^1 1\delta_-^1\rangle$	0.12	0.05	0.02	0.02	0.95	0.16	0.16	1.00	1.00	1.91	0.95	1.79	1.79	1.47
		(0.12	0.05	0.02	0.02	0.95	0.19	0.19	0.99	0.99	1.90	0.95	1.75	1.75	1.42)

[a] Only "valence" electrons are counted.

TABLE 9: Total Energies E (hartree), Equilibrium Bond Distances r_e (Å), Dissociation Energies D_e (kcal/mol), Harmonic Frequencies ω_e and Anharmonicities $\omega_e x_e$ (cm^{-1}), Rotational−Vibrational Constants a_e (10^{-3} cm^{-1}), and Energy Separations T_e (cm^{-1}) of VO^-

method[a]	$-E$	r_e	D_e[b]	ω_e	$\omega_e x_e$	a_e	T_e
			$X^3\Sigma^-$				
CASSCF/B	1017.92659	1.624	140.9	948	8.0	2.4	0.0
MRCI/B	1018.20302	1.623	139.3	974	2.4	2.5	0.0
MRCI+Q/B	1018.22862	1.628	139.3	962	2.3	2.3	0.0
MRCI/BP	1018.20382	1.619	140.5	980	2.7	2.6	0.0
MRCI+Q/BP	1018.22954	1.627	140.7	971	2.4	2.3	0.0
C-MRCI/B	1018.49424	1.612	147.1	985	4.7	3.9	0.0
C-MRCI+Q/B	1018.55829	1.618	146.7	974	2.3	2.4	0.0
C-MRCI/BP	1018.55201	1.611	144.1	988	3.6	3.1	0.0
C-MRCI+Q/BP	1018.62062	1.616	143.9	978	4.5	2.1	0.0
C-MRCI+DKH2/BP	1023.85357	1.609	144.4	990	4.1	3.5	0.0
C-MRCI +DKH2+Q/BP	1023.92218	1.615	144.1	985	2.3	2.6	0.0
RCCSD(T)/B	1018.23553	1.623	139.5				0.0
C-RCCSD(T)/B	1018.58143	1.611	145.3				0.0
C-RCCSD(T)/BP	1018.64655	1.610	142.7	997	4.5	3.2	0.0
C-RCCSD(T)+DKH2/BP	1023.94946	1.608	143.0				0.0
expt[c]			144.2 ± 2.2	900 ± 50			0.0
			$a^5\Pi$				
CASSCF/B	1017.90261	1.601	128.4				6775
RCCSD(T)/BP	1018.20447	1.611	119.7				7098
C-RCCSD(T)/BP	1018.61538	1.601	123.4				6856
C-RCCSD(T)+DKH2/BP	1023.91748	1.602	122.9				7017
expt[c]							6400 ± 200

[a] Internally contracted MRCI and C-MRCI calculations. +Q and DKH2 refer to Davidson correction and to second order Douglas−Kroll−Hess relativistic correction. B and BP refer to Bauschlicher and Balabanov-Petterson basis sets on V; see text. [b] With respect to the ground state fragments, i.e., $V(^4F) + O^-(^2P)$. [c] Reference 15. The "experimental" $D_0(VO^-)$ is obtained through the relation $D_0(VO^-;X^3\Sigma^-) = D_0(VO;X^4\Sigma^-) + EA(VO;X^4\Sigma^-) - EA(O;^3P)$; see text for details.

cation; see vbL diagram (2). According to the latter the VO^+ system is triple bonded in the $^1\Gamma$ state.

According to Table 7 all correlated calculations from C-MRCI down to the highest level predict similar numerical results. At the C-MRCI+DKH2+Q/BP, $D_e = 144$ kcal/mol with respect to $V^+(^3F) + O(^3P)$, and $r_e = 1.547$ Å.

The $^1\Sigma^+$ state, about 2000 cm^{-1} above the $^1\Gamma$, is also triple bonded and can be derived by removing the $4s^1$ ($3\sigma^1$) electron from the $1^2\Sigma^+$ state of neutral VO (see vbL (2)).

The rest of the singlets, $^1\Delta$, $^1\Pi$, and $^1\Phi$ can be traced to the corresponding triplets $^3\Delta$, $^3\Pi$, and $^3\Phi$ of VO^+ but with the two parallel electrons coupled into an (open) singlet. Numerical results are listed in Table 7.

$^5\Pi$, $^5\Sigma^-$. These two quintets are the highest states studied of VO^+, experimentally located 26 858 ± 242 and 30 730 ± 242 cm^{-1} above the $X^3\Sigma^-$ state (see footnote g of Table 7), respectively. Both $^5\Pi$ and $^5\Sigma^-$ are single reference states (Table 8); therefore coupled cluster results can be trusted. Indeed,

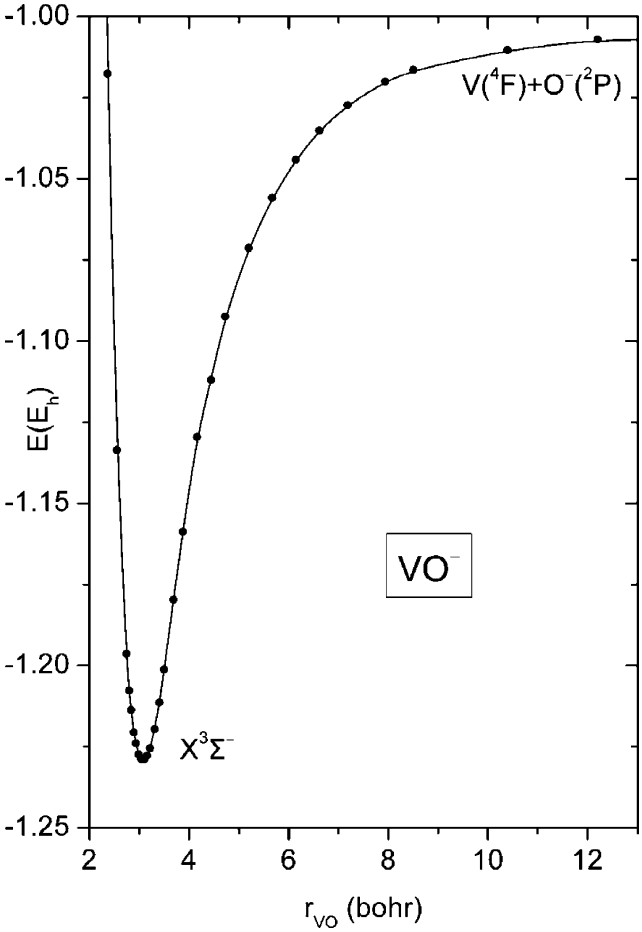

Figure 3. MRCI+Q potential energy curve of the $X^3\Sigma^-$ state of VO^-. Energies are shifted by +1017.0 hartree.

calculated T_e C-RCCSD(T)+DKH2/BP values for both states are in excellent agreement with the above-mentioned experimental T_e results.

The $^5\Pi$ and $^5\Sigma^-$ states can be traced to the $X^4\Sigma^-$ state of VO by detaching a 1π and 2σ electron, respectively, i.e., creating a half π and a half (one electron) σ bond; see the vbL diagram (1). With respect to the $X^4\Sigma^-$ triple bond, the quintets' bond length increases by 0.23 ($^5\Pi$) and 0.16 ($^5\Sigma^-$) Å, reflecting the $2 + {}^1/_2$ bond character.

C. VO^-. $X^3\Sigma^-$, $a^5\Pi$. All existing experimental and theoretical results published on VO^- are given in Table 3. Wu and Wang using photoelectron spectroscopy obtained for the first time the harmonic frequency and the ionization energy of VO^-, hypothesizing a ground state of $^5\Pi$ symmetry.[15] However, the ground state of VO^- is certainly of $^3\Sigma^-$ symmetry according to the recent MR-ACPF calculations of Pykavy and van Wüllen[24] and the present results; see Table 9.

Figure 3 displays the MRCI+Q/B potential energy curve of $X^3\Sigma^-$, correlating to the ground state fragments $V(^4F) + O^-(^2P)$. At the highest level of theory C-MRCI+DKH2+Q/BP (C-RCCSD(T)+DKH2/BP), $D_e = 144.1$ (143.0) kcal/mol, or $D_0 = D_e - ZPE - BSSE = 142$ (141) kcal/mol, in excellent agreement with the experimental value of $D_0 = 144.2 \pm 2.2$ kcal/mol obtained indirectly from the ionization energy of VO^-; see Table 9. Note that the MR-ACPF dissociation energy of ref 24 is rather underestimated by more than 10 kcal/mol. Our ionization energy of VO^- obtained at the RCCSD(T)+DKH2/BP (C-RCCSD(T)+DKH2/BP) level is 1.17 (1.13) eV (see also Table 4 for the EA of $O(^3P)$), in close agreement with the experimental value of Wu and Wang.[15]

TABLE 10: Spin−Orbit Coupling Constants A (cm^{-1}) for VO and VO^+ Multiplets

VO			VO^+	
state	expt[a]	theory[b]	state	theory[b]
$A'^4\Phi$	56.93	58.8	$^3\Phi$	89.1
$A^4\Pi$	35.19	41.8	$^3\Pi$	60.4
$1^2\Delta$	∼158	179.4	$^3\Delta$	87.0
$1^2\Gamma$		4.34	$^5\Pi$	34.3
$B^4\Pi$	63.0	63.8		
$1^2\Phi$	∼66	120.2		

[a] Reference 13. [b] This work.

The CASSCF leading equilibrium configuration and Mulliken atomic populations of the $X^3\Sigma^-$ state of VO^- are

$$|X^4\Sigma^-\rangle \simeq 0.90|1\sigma^2 2\sigma^2 3\sigma^2 1\pi_x^2 1\pi_y^2 1\delta_+^1 1\delta_-^1\rangle$$

$$4s^{1.84}4p_z^{0.15}4p_x^{0.03}4p_y^{0.03}3d_z^{20.63}3d_{xz}^{0.31}3d_{yz}^{0.31}3d_{x^2-y^2}^{1.00}3d_{xy}^{1.00}/_V \quad 2s^{1.87}2p_z^{1.48}2p_x^{1.64}2p_y^{1.64}/_{O^-}$$

A total of about 0.3 e^- are transferred from O^- to V. The bonding, in conformity with the electron distribution above, can be described by the vbL diagram (1) of the $X^4\Sigma^-$ state of VO by adding a single electron to the orbital $4s^1$ ($3\sigma^1$) localized on V.

The first excited state of VO^- is of $^5\Pi$ symmetry, resulting by attaching a single electron to the $4p_\pi$ virtual V orbital of the $X^4\Sigma^-$ state of the neutral species. Wu and Wang recorded a $X' \leftarrow X$ (according to their notation) weak transition with $T = 6400 \pm 200$ cm^{-1} [15] assigned to $a^5\Pi \leftarrow X^3\Sigma^-$ according to our coupled cluster calculations (Table 9). No other experimental results are available for this state. Our CASSCF leading configuration and atomic Mulliken distributions are as follows

$$|a^5\Pi\rangle_{B_1} \simeq 0.95|1\sigma^2 2\sigma^2 3\sigma^1 1\pi_x{}^2 1\pi_y{}^2 2\pi_y{}^1 1\delta_+{}^1 1\delta_-{}^1\rangle$$

$$4s^{1.01}4p_z^{0.10}4p_x^{0.02}4p_y^{0.96}3d_z^{20.58}3d_{xz}^{0.34}3d_{yz}^{0.46}3d_{x^2-y^2}^{1.00}3d_{xy}^{1.00}/_V \quad 2s^{1.87}2p_z^{1.42}2p_x^{1.61}2p_y^{1.55}/_{O^-}$$

As in $X^3\Sigma^-$, $a^5\Pi$ features a triple bond with a total electron transfer of about 0.5 e^- from O^- to V, and a binding energy $D_e = 123$ kcal/mol at $r_e = 1.602$ Å.

D. Spin−Orbit Coupling. For the VO and VO^+ SO multiplets the constant A ($\Delta T = A\Lambda\Sigma$) have been determined at the (valence) MRCI/BP level. The results are shown in Table 10. There are no experimental SO numbers for the VO^+ species. For VO, and with the exception of the $1^2\Phi$ state, our findings can be considered in fair agreement with the experimental results of Merer.[13]

4. Summary

Employing multireference and coupled cluster methods combined with large basis sets, we have obtained the electronic structure for nine ($X^4\Sigma^-$, $\alpha^2\Sigma^-$, $A'^4\Phi$, $1^2\Delta$, $1^2\Gamma$, $A^4\Pi$, $\alpha^2\Sigma^+$, $B^4\Pi$, $1^2\Phi$), 11 ($X^3\Sigma^-$,$^1\Gamma$,$^1\Sigma^+$,$^3\Phi$,$^3\Delta$,$^3\Pi$,$^1\Delta$,$^1\Pi$,$^1\Phi$,$^5\Pi$,$^5\Sigma^-$), and two ($X^3\Sigma^-$, $a^5\Pi$) states of VO, VO^+, and VO^-, respectively. Our main findings can be very briefly summarized as follows

(i) The bonding in VO and VO^+ can be interpreted within the ionic pictures V^+O^- and $V^{2+}O^-$, respectively.

(ii) States $X^4\Sigma^-$, $\alpha^2\Sigma^-$, $1^2\Delta$, $1^2\Gamma$, $\alpha^2\Sigma^+$ of VO, $X^3\Sigma^-$, $^1\Gamma$, $^1\Sigma^+$, $^3\Delta$, $^1\Delta$ of VO^+, and $X^3\Sigma^-$, $a^5\Pi$ of VO^- feature a triple bond character. The rest of the states, except $^5\Sigma^-$ of VO^+, result by breaking a π bond.

(iii) With respect to adiabatic fragments, all states studied (22) can be considered strongly bound, with the highest D_e values 150, 144, and 143 kcal/mol belonging to $X^4\Sigma^-$ (VO), $^1\Gamma$ (VO^+), and $X^3\Sigma^-$ (VO^-), respectively; corresponding r_e values are 1.59, 1.55, and 1.61 Å.

(iv) All singlets and triplets of VO^+ (nine states) are formed by removing an electron from the $4s^1$ ($3\sigma^1$) "nonbonding" orbital localized on the metal.

(v) All our findings are in good to excellent agreement with available experimental results.

Acknowledgment. E.M. expresses his gratitude to Hellenic State Scollarships Foundation (I.K.Y.) for financial support. He is also grateful to Professor Petr Čársky for arranging a 3 month visit at the Heyrovský institute in Prague within the framework of a Marie Curie Fellowship IHP under contract number HPMT-CT-2000-00022.

References and Notes

(1) Merer, A. J.; Huang, G.; Cheung, A. S.-C.; Taylor, A. W. *J. Mol. Spectrosc.* **1987**, *125*, 465 and references therein.

(2) Ram, R. S.; Bernath, P. F.; Davis, S. P.; Merer, A. J. *J. Mol. Spectrosc.* **2002**, *211*, 279. Ram, R. S.; Bernath, P. F. *J. Mol. Spectrosc.* **2005**, *229*, 57 and references therein.

(3) Mahanti, P. *Proc. Phys. Soc. London* **1935**, *47*, 433.

(4) Lagerqvist, A.; Selin, L. *Ark. Fys.* **1956**, *11*, 429; **1957**, *12*, 553.

(5) Berkowitz, J.; Chupka, W. A.; Inghram, M. G. *J. Chem. Phys.* **1957**, *37*, 87.

(6) Coppens, P.; Smoes, S.; Drowart, J. *Trans. Faraday Soc.* **1967**, *63*, 2140.

(7) Kasai, P. H. *J. Chem. Phys.* **1968**, *49*, 4979.

(8) Farber, G. M.; Uy, O. M.; Srivastava, R. D. *J. Chem. Phys.* **1972**, *63*, 2140.

(9) Frantseva, E.; Semenov, G. *A. Tepl. Vys. Temp.* **1969**, *7*, 55.

(10) Jones, R. W.; Gole, J. L. *J. Chem. Phys.* **1976**, *65*, 3800.

(11) Pedley, J. B.; Marshall, E. M. *J. Phys. Chem. Ref. Data* **1983**, *12*, 967.

(12) Balducci, G.; Gigli, G.; Guido, M. *J. Chem. Phys.* **1983**, *79*, 5616.

(13) Merer, A. *J. Annu. Rev. Phys. Chem.* **1989**, *40*, 407 and references therein.

(14) Suenram, R. D.; Fraser, G. T.; Lovas, F. J.; Gillies, C. W. *J. Mol. Spectrosc.* **1991**, *148*, 114.

(15) Wu, H.; Wang, L. S. *J. Chem. Phys.* **1998**, *108*, 5310.

(16) Cheung, A. S.-C.; Hajigeorgiou, P. G.; Huang, G.; Huang, S. Z.; Merer, A. J. *J. Mol. Spectrosc.* **1994**, *163*, 443.

(17) Carlson, K. D.; Moser, C. *J. Chem. Phys.* **1966**, *44*, 3259.

(18) Bausclicher, C. W., Jr.; Langhoff, S. R. *J. Chem. Phys.* **1986**, *85*, 5936.

(19) Dolg, M.; Wedig, U.; Stoll, H.; Preuss, H. *J. Chem. Phys.* **1987**, *86*, 2123.

(20) Bausclicher, C. W., Jr.; Maitre, P. *Theor. Chim. Acta* **1995**, *90*, 189.

(21) Gutsev, G. L.; Rao, B. K.; Jena, P. *J. Phys. Chem. A* **2000**, *104*, 5374.

(22) Brocławik, E.; Borowski, T. *Chem. Phys. Lett.* **2001**, *339*, 433.

(23) Calatayud, M.; Silvi, B.; Andrés, J.; Beltrán, A. *Chem. Phys. Lett.* **2001**, *333*, 493.

(24) Pykavy, M.; van Wüllen, C. *J. Phys. Chem. A* **2003**, *107*, 5566.

(25) Aristov, N.; Armentrout, P. B. *J. Am. Chem. Soc.* **1984**, *106*, 4065.

(26) Dyke, J. M.; Gravenor, B. W. J.; Hastings, M. P.; Morris, A. *J. Phys. Chem.* **1985**, *89*, 4613.

(27) Aristov, N.; Armentrout, P. B. *J. Phys. Chem.* **1986**, *90*, 5135.

(28) Clemmer, D. E.; Elkind, J. L.; Aristov, N.; Armentrout, P. B. *J. Chem. Phys.* **1991**, *95*, 3387.

(29) Brümmer, M.; Kaposta, C.; Santambrogio, G.; Asmis, K. *J. Chem. Phys.* **2003**, *119*, 12700.

(30) Carter, E. A.; Goddard, W. A., III. *J. Phys. Chem.* **1988**, *92*, 2109.

(31) Brocławik, E. *Int. J. Quantum Chem.* **1995**, *56*, 779.

(32) Kretzschmar, I.; Schröder, D.; Schwartz, H.; Rue, C.; Armentrout, P. B. *J. Phys. Chem. A* **1998**, *102*, 10060.

(33) Nakao, Y.; Hirao, K.; Taketsugu, T. *J. Chem. Phys.* **2001**, *114*, 7935.

(34) Vyboishchikov, S. F.; Sauer, J. *J. Phys. Chem. A* **2000**, *104*, 10913.

(35) Neumark, D. M.; Lykke, K. R.; Anderson, T.; Lineberger, W. C. *Phys. Rev. A* **1983**, *32*, 1890.

(36) Bausclicher, C. W., Jr. *Theor Chim. Acta* **1995**, *92*, 183.

(37) Dunning, T. H., Jr. *J. Chem. Phys.* **1989**, *90*, 1007.

(38) Balabanov, N. B.; Peterson, K. A. *J. Chem. Phys.* **2005**, *123*, 064107.

(39) Werner, H.-J.; Knowles, P. J. J. *Chem. Phys.* **1988**, *89*, 5803. Knowles, P. J.; Werner, H.-J. *Chem. Phys. Lett.* **1988**, *145*, 514. Werner, H.-J.; Reinsch, E. A. *J. Chem. Phys.* **1982**, *76*, 3144. Werner, H.-J. *Adv. Chem. Phys.* **1987**, L**1988**, *XIX*, 1.

(40) Raghavachari, K.; Trucks, G. W.; Pople, J. A.; Head-Gordon, M. *Chem. Phys. Lett.* **1989**, *157*, 479. Bartlett, R. J.; Watts, J. D.; Kucharski, S. A.; Noga, J. *Chem. Phys. Let.* **1990**, *165*, 513; **1990**, *167*, 609. E. Knowles, P. J.; Hampel, C.; Werner, H.-J. *J. Chem. Phys.* **1993**, *99*, 5219; **2000**, *112*, 3106E.

(41) Douglas, M.; Kroll, N. M. *Ann. Phys.* **1974**, *82*, 89. Hess, B. A. *Phys. Rev. A.* **1985**, *32*, 756. *Ann. Phys.* **1986**, *33*, 3742. Jansen, G.; Hess, B. A. *Ann. Phys.* **1989**, *39*, 6016.

(42) Boys, S. F.; Bernardi, F. *Mol. Phys.* **1970**, *19*, 553. Liu, B.; McLean, A. D. *J. Chem. Phys.* **1973**, *59*, 4557. Jansen, H. B.; Ros, P. *Chem. Phys. Lett.* **1969**, *3*, 140.

(43) Docken, K.; Hinze, J. *J. Chem. Phys.* **1972**, *57*, 4928. Werner, H.-J.; Meyer, W. *J. Chem. Phys.* **1981**, *74*, 5794.

(44) MOLPRO, version 2002.6, is a package of ab initio programs designed by H.-J. Werner, P. J. Knowles, R. D. Amos, et al. MOLPRO, version 2006.1, a package of ab initio programs, H.-J. Werner, P. J. Knowles, R. Lindh, F. R. Manby, M. Schütz, and others, see http://www.molpro.net.

(45) Ralchenko, Yu.; Jou, F.-C.; Kelleher, D.E.; Kramida, A.E.; Musgrove, A.; Reader, J.; Wiese, W.L.; Olsen, K. NIST Atomic Spectra Database (version 3.1.0); http://physics.nist.gov/asd3; National Institute of Standards and Technology: Gaithersburg, MD, October 2006

(46) Tzeli, D.; Mavridis, A. *J. Chem. Phys.* **2003**, *118*, 4984. *J. Chem. Phys.* **2003**, *122*, 056101.